UNDERSTANDING THE IMPORTANCE OF TWIGS IN NON-DESTRUCTIVE TREE MODELING

By

Aidan Morales

A THESIS

Submitted to
Michigan State University
in partial fulfillment of the requirements
for the degree of

Forestry – Master of Science

2024

ABSTRACT

This thesis presents a new method, Real Twig, to correct volume overestimation in small branches and twigs in quantitative structure models (QSM). Twigs are the smallest above-ground woody structure on a tree and contain delicate tissues used in growing new woody material, leaves for photosynthesis, and fruits for reproduction. Remote sensing with terrestrial laser scanning (TLS) can capture the unique branching structure of trees with millions of indirect measurements stored as a three-dimensional point cloud. QSMs are cylinder models fit to tree point clouds that define a tree's branching structure as a topological network of cylinders, providing non-destructive estimates of total tree volume and surface area. However, TLS cannot accurately resolve fine details in a tree, specifically twigs, due to physical limitations of TLS sensors, causing the twigs to be much larger in the point cloud than they are in the actual tree. Since QSMs are built from point clouds, the twigs represent a large source of whole-tree volume overestimation directly proportional to the total twig volume in the tree, with error often double the tree's actual volume, even with the current best correction methods applied.

The thesis results show the Real Twig method drastically outperforms all the current best correction methods, by combining direct twig diameter measurements with dynamic taper models to produce visually realistic QSMs that overcome deficiencies in TLS sensor technology. The results show a drastic reduction in QSM volume overestimation, with total tree volume consistently within ± 10% of the real tree. The results also show that TLS data collection must be optimized around the species-specific twig diameter measurement. Finally, a detailed description of the method, a novel database of twig diameter measurements, and tools for QSM visualization, manipulation, and the calculation of QSM-based tree metrics, can be found in an open source R package called *rTwig*.

ACKNOWLEDGEMENTS

First, I would like to thank my advisor, Dr. David W. MacFarlane, throughout all my time as a forestry student at Michigan State University. Dr. MacFarlane not only provided me guidance in my studies and research, but also instilled in me the importance of quality work, which stems from a desire to understand the world around us, not least of which is a love for real trees. I would also like to thank my committee members, Dr. Andrew O. Finley, and Dr. Scott Stark for their valuable feedback and suggestions in my thesis.

I also extend thanks to Michigan State University, the USDA Forest Service, and the USDA Forest Inventory and Analysis Program, whose joint venture funded this research. Additionally, I extend thanks to the MSU Graduate School for funding my first year of research.

I would also like to extend a very special thanks to both Samuel Clark and Dr. Georgios Arseniou for all their guidance and friendship throughout the years. Finally, I would like to thank my family and all my friends in the forestry community for putting up with my all too many obsessions about trees, forests, and everything else.

TABLE OF CONTENTS

CHAPTER 1

INTRODUCTION

1.1 The Importance of Twigs

Twigs are the smallest above-ground woody structure on a tree and are responsible for many important biological functions, including the housing of meristematic tissue used for new twig growth, leaf production for photosynthesis, fruit production for reproduction, and protection from the elements during the dormant season (Flint, 1972; Wiegand, 1906). Twigs have been infrequently studied for functional and structural traits in different species (Rosell et al., 2015; Yao et al., 2015), their importance in supporting diverse plant communities (Lamit et al., 2014), or indirectly studied in general tree allometry and fractal architecture as a function of branch length or volume (Koyama et al., 2017; MacFarlane et al., 2014). Due to the difficulty of measuring twigs directly, which can number into the thousands on a single branch and are considered the key to understanding tree growth and structure (Wilson, 1989), little research has been conducted on the importance of twig diameters across different species and how this relates to branch architecture and branch tapering. Given the importance of twigs, it is critical to improve methods to not only measure twigs in a consistent and biologically meaningful way, but also consider twigs in holistic tree modeling.

1.2 Remote Sensing and Twigs

Terrestrial laser scanning (TLS), a form of active remote sensing capable of recording millions of data points at a single scan location, has cemented itself as an efficient way to quantify forest structure without the need for destructive measurements (Calders et al., 2020; Malhi et al., 2018). Following efficient scanning patterns with an appropriate TLS sensor during optimal environmental conditions can yield highly detailed point clouds of individual trees and forest stands as a snapshot in time, including branches and twigs > 30 meters above the ground in the upper canopy (Wilkes et al., 2017). Since tree point clouds are captured as a snapshot in time, the growth or loss of twigs and branches can be consistently monitored over time with repeated scans in known locations (Calders et al., 2020; Newnham et al., 2015). Tracking changes in new twig growth and secondary growth with TLS can improve on existing allometric models for above ground biomass and carbon estimation (Calders et al., 2022; Kaasalainen et al., 2014; Muumbe et al., 2021).

1.3 Quantitative Structure Models and Twigs

Quantitative structure models (QSM) are used to transform point clouds of trees into an efficient format for quantitative analysis. QSMs represent the topology of a tree as a connected network of cylinders, with the cylinder length, orientation, and radius estimated directly from the input point cloud (Fan et al., 2020; Hackenberg et al., 2015; Raumonen et al., 2013; Wilkes et al., 2021; Yang et al., 2024). While TLS can precisely and efficiently measure points on trees, the points that are recorded on small diameter parts of a tree, such as small branches and twigs, are overestimated to varying degrees depending on the TLS sensor used. The three main reasons for overestimation include wind noise, beam divergence, and co-registration errors (Demol et al., 2022; Lau et al., 2018; Seidel et al., 2012; Wilkes et al., 2017, 2021), all of which are current limitations of TLS sensor technology.

When small branch and twig points (approximately ≤ 5–7 centimeters in diameter) are used in QSMs, the resulting cylinder radii are overinflated, leading to total tree volume overestimation several orders of magnitude larger than known reference volume (Demol et al., 2021, 2022; Wilkes et al., 2021). Any metrics that include QSM small branch and twig cylinders, such as volume, surface area, and branch taper, will be incorrect and unrealistic. There have been several attempts to correct and mitigate this problem, including mathematical taper functions and allometric scaling theory (Hackenberg & Bontemps, 2023; Raumonen et al., 2013; Wilkes et al., 2021), but such solutions either include the overestimated cylinders in the taper function, or exclude real information about twig sizes to generalize the correction for all tree growth forms and species. Currently, no satisfactory method exists to overcome small branch and twig overestimation from point clouds using QSMs.

1.4 Thesis Intent and Outline

This thesis seeks to explore real twig measurements to better understand the limitations of current TLS technology and its ability to accurately resolve twigs from tree point clouds. We collected as many real measurements on trees as possible to better inform modeled branch taper from quantitative structure models. The goal was to provide a systematic and unbiased method to measure tree twigs across a wide range of genera and use these twig measurements to improve non-destructive volume estimates of trees with QSMs. We wanted to create a method to model QSM branch tapering that is holistic and non-statistical by incorporating tree-specific allometry and real measurements (i.e., the twig diameter measurements) directly into our model.

Chapter 1 is the introductory chapter and lays the foundation of why twigs are important and describes the issues associated with measuring twigs directly. Chapter 1 also describes the background on inflated twig diameters from remote sensing, due to technological limitations of measuring twigs indirectly, and the volume overestimation associated with using these measurements in QSMs. Chapter 2 provides a systematic and unbiased protocol for measuring twig diameters and describes our Real Twig method. Chapter 2 also provides best practices for QSM generation, presents our findings using the Real Twig method, and discusses why twig measurements of real trees are critical for precise and accurate QSM volume estimates. Chapter 3 describes our R package, *rTwig*, which contains our database of twig diameter measurements and tools for correcting volume overestimation in QSMs. Chapter 3 also provides detailed examples on how to use the package, including implications of the method. Finally, Chapter 4 discusses the implications of the Real Twig method and how laser scanning methods and sensor technology affects indirect twig measurement. We also discuss best practices for laser scanning trees and twigs based on our findings and current literature.

REFERENCES

Calders, K., Adams, J., Armston, J., Bartholomeus, H., Bauwens, S., Bentley, L. P., Chave, J., Danson, F. M., Demol, M., Disney, M., Gaulton, R., Krishna Moorthy, S. M., Levick, S. R., Saarinen, N., Schaaf, C., Stovall, A., Terryn, L., Wilkes, P., & Verbeeck, H. (2020). Terrestrial laser scanning in forest ecology: Expanding the horizon. *Remote Sensing of Environment, 251*, 112102. https://doi.org/10.1016/J.RSE.2020.112102

Calders, K., Verbeeck, H., Burt, A., Origo, N., Nightingale, J., Malhi, Y., Wilkes, P., Raumonen, P., Bunce, R. G. H., & Disney, M. (2022). Laser scanning reveals potential underestimation of biomass carbon in temperate forest. *Ecological Solutions and Evidence*, *3*(4). https://doi.org/10.1002/2688-8319.12197

Demol, M., Calders, K., Verbeeck, H., & Gielen, B. (2021). Forest above-ground volume assessments with terrestrial laser scanning: a ground-truth validation experiment in temperate, managed forests. *Annals of Botany*, *128*(6), 805–819. https://doi.org/10.1093/aob/mcab110

Demol, M., Wilkes, P., Raumonen, P., Krishna Moorthy, S., Calders, K., Gielen, B., & Verbeeck, H. (2022). Volumetric overestimation of small branches in 3D reconstructions of & Fraxinus excelsior; *Silva Fennica*, *56*(1), 10550. https://doi.org/10.14214/sf.10550

Fan, G., Nan, L., Dong, Y., Su, X., & Chen, F. (2020). AdQSM: A New Method for Estimating Above-Ground Biomass from TLS Point Clouds. *Remote Sensing*, *12*(18), 3089. https://doi.org/10.3390/rs12183089

Flint, H. L. (1972). Cold Hardiness of Twigs of Quercus Rubra L. As a Function of Geographic Origin. *Ecology*, *53*(6), 1163–1170. https://doi.org/10.2307/1935430

Hackenberg, J., & Bontemps, J.-D. (2023). Improving quantitative structure models with filters based on allometric scaling theory. *Applied Geomatics*, *15*(4), 1019–1029. https://doi.org/10.1007/s12518-023-00537-4

Hackenberg, J., Spiecker, H., Calders, K., Disney, M., Raumonen, P., Hyyppä, J., Liang, X., & Puttonen, E. (2015). *SimpleTree-An Efficient Open Source Tool to Build Tree Models from TLS Clouds*. *6*, 4245–4294. https://doi.org/10.3390/f6114245

Kaasalainen, S., Krooks, A., Liski, J., Raumonen, P., Kaartinen, H., Kaasalainen, M., Puttonen, E., Anttila, K., & Mäkipää, R. (2014). Change Detection of Tree Biomass with Terrestrial Laser Scanning and Quantitative Structure Modelling. *Remote Sensing*, *6*(5), 3906–3922. https://doi.org/10.3390/rs6053906

Koyama, K., Yamamoto, K., & Ushio, M. (2017). A lognormal distribution of the lengths of terminal twigs on self-similar branches of elm trees. *Proceedings of the Royal Society B: Biological Sciences*, *284*(1846), 20162395. https://doi.org/10.1098/rspb.2016.2395

Lamit, L. J., Lau, M. K., Sthultz, C. M., Wooley, S. C., Whitham, T. G., & Gehring, C. A. (2014). Tree genotype and genetically based growth traits structure twig endophyte communities. *American Journal of Botany*, *101*(3), 467–478. https://doi.org/10.3732/ajb.1400034

Lau, A., Bentley, L. P., Martius, C., Shenkin, A., Bartholomeus, H., Raumonen, P., Malhi, Y., Jackson, T., & Herold, M. (2018). Quantifying branch architecture of tropical trees using terrestrial LiDAR and 3D modelling. *Trees*, *32*(5), 1219–1231. https://doi.org/10.1007/s00468-018-1704-1

MacFarlane, D. W., Kuyah, S., Mulia, R., Dietz, J., Muthuri, C., & Van Noordwijk, M. (2014). Evaluating a non-destructive method for calibrating tree biomass equations derived from tree branching architecture. *Trees*, 807–817. https://doi.org/10.1007/s00468-014-0993-2

Malhi, Y., Jackson, T., Patrick Bentley, L., Lau, A., Shenkin, A., Herold, M., Calders, K., Bartholomeus, H., & Disney, M. I. (2018). New perspectives on the ecology of tree structure and tree communities through terrestrial laser scanning. *Interface Focus*, *8*(2), 20170052. https://doi.org/10.1098/rsfs.2017.0052

Muumbe, T. P., Baade, J., Singh, J., Schmullius, C., & Thau, C. (2021). Terrestrial Laser Scanning for Vegetation Analyses with a Special Focus on Savannas. *Remote Sensing*, *13*(3), 507. https://doi.org/10.3390/rs13030507

Newnham, G. J., Armston, J. D., Calders, K., Disney, M. I., Lovell, J. L., Schaaf, C. B., Strahler, A. H., & Danson, F. M. (2015). Terrestrial Laser Scanning for Plot-Scale Forest Measurement. *Current Forestry Reports*, *1*(4), 239–251. https://doi.org/10.1007/s40725-015-0025-5

Raumonen, P., Kaasalainen, M., Akerblom, M., Kaasalainen, S., Kaartinen, H., Vastaranta, M., Holopainen, M., Disney, M., & Lewis, P. (2013). Remote Sensing Fast Automatic Precision Tree Models from Terrestrial Laser Scanner Data. *Remote Sens*, *5*, 491–520. https://doi.org/10.3390/rs5020491

Rosell, J. A., Castorena, M., Laws, C. A., & Westoby, M. (2015). Bark ecology of twigs vs. main stems: functional traits across eighty-five species of angiosperms. *Oecologia*, *178*(4), 1033–1043. https://doi.org/10.1007/s00442-015-3307-5

Seidel, D., Fleck, S., & Leuschner, C. (2012). Analyzing forest canopies with ground-based laser scanning: A comparison with hemispherical photography. *Agricultural and Forest Meteorology*, *154–155*, 1–8. https://doi.org/10.1016/j.agrformet.2011.10.006

Wiegand, K. M. (1906). Some Studies Regarding the Biology of Buds and Twigs in Winter. *Botanical Gazette*, *41*(6), 373–424. https://doi.org/10.1086/328871

Wilkes, P., Lau, A., Disney, M., Calders, K., Burt, A., Gonzalez de Tanago, J., Bartholomeus, H., Brede, B., & Herold, M. (2017). Data acquisition considerations for Terrestrial Laser Scanning of forest plots. *Remote Sensing of Environment*, *196*, 140–153. https://doi.org/10.1016/j.rse.2017.04.030

Wilkes, P., Shenkin, A., Disney, M., Malhi, Y., Bentley, L. P., & Vicari, M. B. (2021). Terrestrial laser scanning to reconstruct branch architecture from harvested branches. *Methods in Ecology and Evolution*, *12*(12), 2487–2500. https://doi.org/10.1111/2041-210X.13709

Wilson, B. F. (1989). Tree branches as populations of twigs. *Canadian Journal of Botany*, *67*(2), 434–442. https://doi.org/10.1139/b89-060

Yang, W., Wilkes, P., Vicari, M. B., Hand, K., Calders, K., & Disney, M. (2024). Treegraph: Tree Architecture from Terrestrial Laser Scanning Point Clouds. *Remote Sensing in Ecology and Conservation*. https://doi.org/10.1002/rse2.399

Yao, F., Chen, Y., Yan, Z., Li, P., Han, W., & Fang, J. (2015). Biogeographic Patterns of Structural Traits and C:N:P Stoichiometry of Tree Twigs in China's Forests. *PLOS ONE*, *10*(2), e0116391. https://doi.org/10.1371/journal.pone.0116391

CHAPTER 2

REDUCING TREE VOLUME OVERESTIMATION IN QUANTITATIVE STRUCTURE MODELS USING MODELED BRANCH TOPOLOGY AND DIRECT TWIG MEASUREMENTS

Abstract

Quantitative Structure Models (QSMs) are fit to tree point clouds to represent the topology of trees as a network of cylinders. QSMs allow for the calculation of metrics difficult to measure without destructive sampling, including total tree volume. Current limitations in TLS technology make small branches difficult to accurately resolve, overestimating small branch volume in QSMs, which can translate into overestimation of tree biomass. We present a new method called Real Twig to correct overestimated small branch and twig cylinders in QSMs. Real Twig differs from current methods by using twig diameters measured directly from corresponding tree species to model a unique taper for every path in the QSM using the QSM's inherent branching topology, without relying on predefined mathematical or allometric relationships. To test Real Twig, we generated QSMs for different sets of trees that had detailed dry mass and density measurements obtained via felling after scanning. QSM-based biomass estimates were obtained by multiplying the tree's QSM-based volume estimate by the tree's specific basic density value. We trained our method with high-quality data consisting of five northern red oak (*Quercus rubra L.*) and five red maple (*Acer rubrum L.*) trees, using two different versions of TreeQSM, a widely used algorithm for generating QSMs. We further tested our method on three publicly available datasets, including managed forests and large tropical trees, collected with both phase shift or time-of-flight sensors. QSMs corrected with our Real Twig method showed a very large improvement in tree biomass estimation, with a relative mean error of -1.2%, a relative root mean square error of 10.5%, and a concordance correlation coefficient of 0.999, compared to a relative mean error of 76.8%, a relative root mean square error of 48.7%, and a concordance correlation coefficient of 0.982, when using the standard outputs of TreeQSM.

2.1 Introduction

Accurate estimates of total above ground biomass (AGB) are important to understand how forests store carbon long term and respond to changes in atmospheric carbon dioxide (Houghton, 2005). Since whole trees cannot be weighed while standing for AGB, allometric equations are used to estimate AGB from simple variables, such as the diameter at breast height (DBH) or total height of a tree (Vorster et al., 2020). The underlying data for allometric equations typically requires destructive sampling, where trees are cut down and entirely weighed to fit a predictive equation covering a range of size classes and growing conditions (MacFarlane et al., 2014). However, destructive sampling is not only time consuming and expensive, but is often not feasible for rare, threatened, or endangered tree species (Frank et al., 2019).

While there are some non-destructive approaches to estimate AGB (MacFarlane et al., 2014; Montès et al., 2000), terrestrial laser scanning (TLS) has emerged as an efficient alternative to destructive sampling over the past decade (Arseniou et al., 2023; Calders et al., 2015a; Demol et al., 2022a; Disney et al., 2018; Holopainen et al., 2012; Stovall et al., 2017). With TLS, single trees or forest stands can be captured as a series of three-dimensional coordinates in space, known as a point cloud, enabling the computation of metrics traditionally difficult or impossible to capture otherwise (Calders et al., 2020). Point clouds capture a snapshot of a tree or forest stand at a specific point in time, making TLS well suited for forest inventory (Liang et al., 2016). Since the technical measurement biases and limitations unique to different laser scanning sensors are well documented and TLS can represent trees holistically with millions of unique data points, TLS may be less susceptible to errors when compared to traditional forest measurements (Calders et al., 2018; Calders et al., 2020). Moreover, because large trees are often missing from destructive sampling data (Weiskittel et al., 2015), TLS may be more suitable to develop allometric models across a wide range of tree sizes and forest types (Calders et al., 2022).

If the volume of a tree can be computed from a point cloud, AGB can be estimated non-destructively, by multiplying tree volume by a measured or published tree (wood and bark) density value (Arseniou et al., 2023). There are multiple approaches to calculate the volume of a tree from its point cloud. One approach well suited for conifers is the Outer Hull Model, where the point cloud is voxelized, woody material separated, and volume summed for the main stem and branch components (Stovall et al., 2017).

A widely used approach is using a Quantitative Structure Model (QSM) (Fan et al., 2020; Hackenberg et al., 2015a; Raumonen et al., 2013; Yang et al., 2024), which uses geometric primitives to represent the tree's topology from the point cloud. Using cylinders as a fundamental building block allows detailed branch structural metrics, surface area, volume, and other metrics to be easily calculated (Åkerblom et al., 2017; Arseniou et al., 2021b; Terryn et al., 2020), and individual main stem and branch volumes to be compared to reference measurements to assess QSM accuracy. One QSM approach is breaking the point cloud into small segments of points and using neighbor relationships to identify connected portions and bifurcations, where a new branch and branch order begin at each bifurcation, and cylinders are fit to the points with least squares iteration on a per branch basis (Raumonen et al., 2013). Alternate QSM approaches may define the tree's topology with a sphere following system to identify connected portions and bifurcations (Hackenberg et al., 2015a) or use the point cloud itself to create an underlying skeleton of nodes and internodes representing the tree's branching structure (Yang et al., 2024). Regardless of the method used, the accuracy of a QSM is always limited by the quality of the point cloud data. Higher quality point clouds allow for better QSM topology and vice versa.

When carefully modeled with proper topology, QSMs can show good agreement with their reference destructive sampling data (Arseniou et al., 2023; Burt et al., 2021; Calders et al., 2015a; Demol et al., 2021b; Momo Takoudjou et al., 2018). However, current TLS technology struggles to accurately capture small branches and twigs in trees, due to beam divergence (the widening of the laser beam footprint with increasing distance from the scanner), occlusion, wind effects, and co-registration errors (Disney et al., 2018; Wilkes et al., 2017, 2021). QSMs typically reconstruct oversized small branches and twigs, leading to a large volume overestimation, often doubling the actual volume in branches < 7 cm (Demol et al., 2021a; Demol et al., 2022b; Hackenberg et al., 2015b; Wilkes et al., 2021). These TLS sensor limitations are exacerbated as distance from the sensor increases, such that a decrease in point cloud quality and poor resolution of fine branching structures causes QSM volume and radii overestimation to increase drastically for small branches (Morhart et al., 2024). Any bias in QSM volume translates directly to inaccuracy in biomass estimation.

There are several current approaches to deal with this small branch overestimation problem. The first is to simply discard branches with a base cylinder diameter less than or equal to the error threshold (Demol et al., 2021a; Gonzalez de Tanago et al., 2018). This approach works well when only large branches are of interest, but necessarily omits part of the tree for total tree volume or AGB estimates. Another approach is an allometric statistical correction (Hackenberg et al., 2015a; Hackenberg & Bontemps 2023), where the cylinder radius is plotted against a strong independent predictor variable, and a power function is fit to identify overestimated cylinder radii with a user-defined confidence interval; any cylinder outside of this interval is considered an outlier and the overestimated cylinder radii are corrected by moving them to the predicted line. This generalized allometric correction approach assumes the allometry of the tree is self-similar throughout all parts of the tree. This assumption is unlikely to be true, and it forces the tree to have a specific mathematical shape, regardless of whether this reflects the real taper in different parts of the tree. A more refined solution was developed by Raumonen et al. (2013), which adjusts the taper of each branch locally by constraining cylinders in branches to be smaller than those in their parent branches, usually combined with a parabolic model fit to cross-sections of the branch, which forces the branch to taper towards a fixed minimum constraint. This has been employed in other studies with varying minimum constraint sizes, with similar results (see, e.g., Wilkes et al., 2021). This approach significantly improves branch tapering, but it does not constrain the branch to be realistic in size or consider the general allometry of the tree (unlike the allometric approach described above) and can sometimes modify the radii of larger cylinders that do not need correction.

Here, we present a new method called 'Real Twig' to correct inherent QSM small branch and twig overestimation biases. The motivation behind Real Twig is to provide QSMs that are not only realistic looking, but also have precise and accurate tree metrics. If the QSM closely resembles its real-life counterpart, accurate tree metrics, such as volume, surface area, length, and biomass, will naturally follow. We designed Real Twig with only one assumption about tree architecture, namely that the twig is the smallest above ground woody building block of any tree species. To this end, Real Twig improves upon previous approaches by correcting every cylinder in a QSM using an allometric taper model uniquely fit to each path in a tree's branching network, constrained by the actual twig diameter measurement specific to the given tree species. Once the twig diameter is given, our method is entirely automated, adaptable for different workflows, and can be run on any QSM that provides topological relationships between cylinders. The results of this study tested the effectiveness of combining species-specific, direct twig measurements and dynamic taper models throughout a QSM to overcome deficiencies in current TLS sensor technology for use in tree modeling.

2.2 Methods

2.2.1 Real Twig

Real Twig differs from other QSM correction methods (described above) by using parts of a QSM that are well modeled and adequately covered with laser points (e.g., large branches and their cylinders) to inform the taper of poorly modeled parts (e.g., small branches and twigs) down to the twig level. Unlike the approach of Hackenberg et al. (2015a), this approach does not assume that every part of the tree tapers in the same way. Unlike the approach of Raumonen et al. (2013), which uses only local information to adjust the taper of each branch, Real Twig models every 'path' in a QSM from the base cylinder to each twig tip (Fig. 2.1b), where the largest part of the tree is its base, and the smallest part is a twig that ends a path. Real Twig uses a monotonic generalized additive model (GAM), which allows it to automatically incorporate species-specific twig allometry into our corrected QSMs. The total number of paths is always equal to the total number of twigs in the QSM, which can range from a few hundred for small trees, to thousands in large trees. Twig radii can be easily and quickly measured on a tree and provide tree or species-specific information to correct poorly modeled cylinder radii in a QSM. Detailed step-by-step instructions for applying the Real Twig method and visualized results are outlined in Figure 2.1.

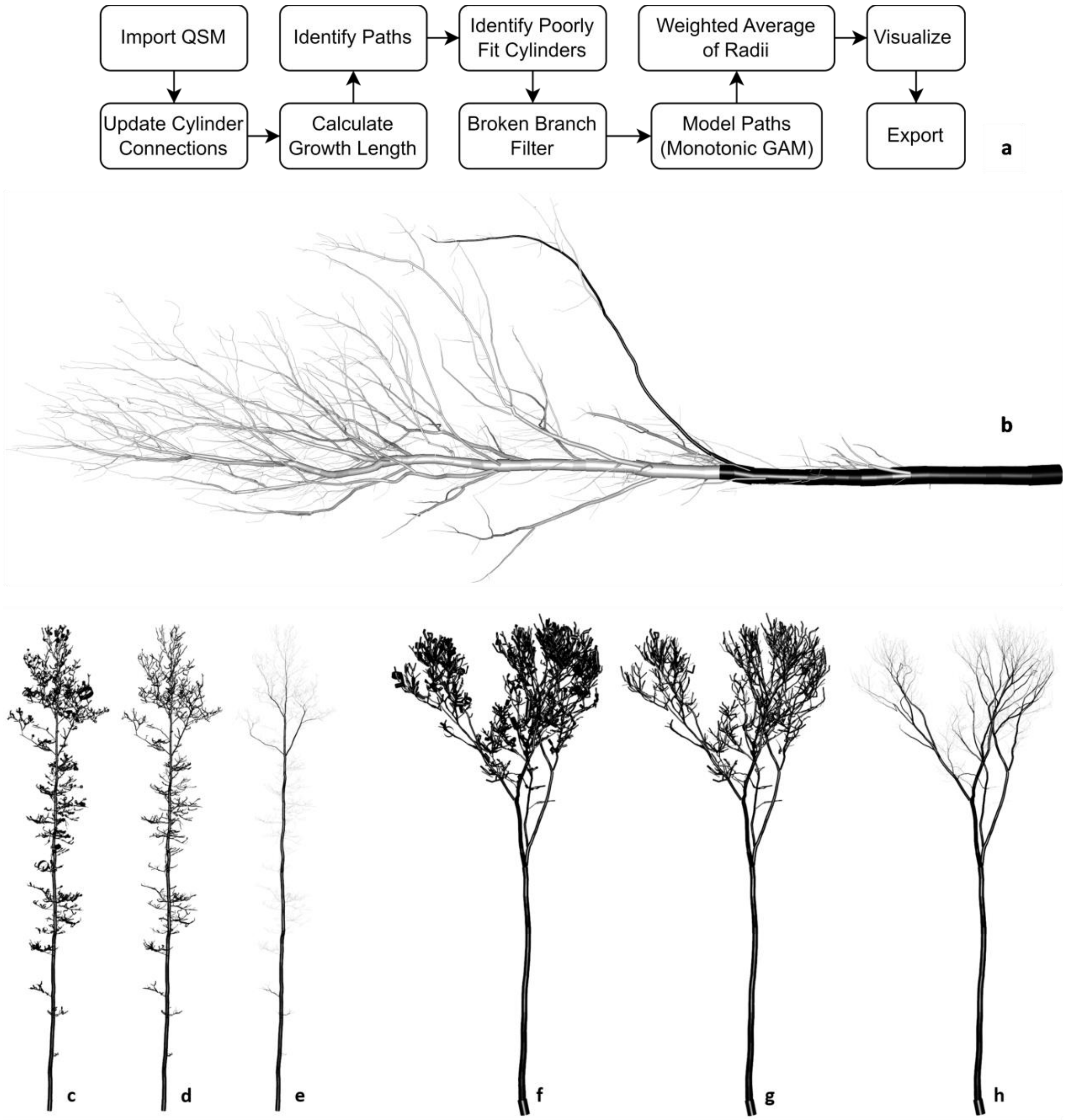

Figure 2.1 (a) Flowchart of the Real Twig processing steps and (b) an illustration of a Quantitative Structural Model (QSM) for a European ash tree with a single "path" highlighted in black. A path starts at the basal cylinder in the QSM and proceeds to a terminal twig; the number of paths in the tree is equal to the number of twigs. (c) & (f) QSM cylinders without modifications for a sessile oak and northern red oak tree. (d) & (g) QSM cylinders with TreeQSM's standard parent-child and parabolic tapering correction. (e) & (h) TreeQSM cylinders corrected with Real Twig.

The first step of the Real Twig method (see flowchart in Fig. 2.1a) is to ensure all parent-child cylinder relationships are consecutively defined. This ensures that all paths in the tree, from the base to each branch tip, can be successfully traced. We set the first cylinder (the base of the tree) to have an index of one, and all the child cylinders are numbered in consecutive order based on their parent-child relationships. The result is a QSM where the first cylinder index is the base of the main stem, and the last cylinder index is equal to the total number of cylinders in the QSM. We follow a similar procedure for the branches, where the main stem is defined as branch one, and the rest of the branches are numbered consecutively until the last branch is reached. Our definition of orders and branches follows the approach of TreeQSM, where a new branch begins at a new branch order and ends at a twig tip (Raumonen et al., 2013).

Next, we calculate the 'growth length' of each cylinder, which is the length of a given parent cylinder, plus the length of every child cylinder supported by the parent cylinder (Hackenberg et al., 2015a; Hackenberg & Bontemps, 2023). We use the growth length parameter because it can be matched to real measurements on a tree and does not contain any of the cylinder radii errors we are trying to correct, unlike the 'growth volume', employed by Hackenberg et al. (2015a). Growth length also identifies all twigs in a QSM, which will always have a growth length equal to their cylinder length. We calculate growth length recursively for each cylinder using the R (R Core Team, 2023) implementation of the *igraph* software package (Csárdi et al., 2023). For every cylinder we recursively identify all its child cylinders and sum the length of these cylinders to get each cylinder's growth length.

Next, we identify all paths in the QSM, from the base of the tree to each branch tip (Fig. 2.1b), using the *igraph* software package (Csárdi et al., 2023). The total number of paths in a QSM is always equal to the number of twig cylinders. Before we can model the path taper, we need to remove all poorly modeled cylinders (e.g., Fig. 2.1 c, f), whose radii will influence the GAM taper. For every cylinder in each branch order in the path, we use the following filter.

$$Y_1 = a \,/\, b \,/\, (c + 1)$$

$$Y_2 = \frac{\log\,(b)}{a^2}$$

$$Y_3 = \frac{a^2}{\log\,(b)}$$

$$lower = IQR(Y_x) * 1.5 - Q1$$

$$upper = IQR(Y_x) * 1.5 + Q3$$

$$I = 0, if\ Y_x\ \geq lower\ and\ Y_x\ \leq upper, else\ I = 1$$

where *a* is the cylinder radius, *b* is the cylinder growth length, *c* is the branch order, Y_1 is the general cylinder pass, Y_2 is the small cylinder pass, Y_3 is the large cylinder pass, *Q1* is the first quartile, *Q3* is the third quartile, *I* is a binary index, where 0 is a good fit, and 1 is a poor fit, and all poor fits are removed before the next Y_x filter. Only the cylinders that remain after this filter are used in the next step. Y_2 and Y_3 are done separately for each branch order along the path, while Y_1 is done along the entire path.

Next, we run all the remaining good fit cylinders through a recursive taper filter, where the i^{th} cylinder in the path can only be *1 / sqrt(i)* larger than all cylinders before it in the path. This allows for greater radii variation at the base of the path, and a very tight taper as we approach the twig. The cylinders that remain following the taper filter are used to fit a monotonic GAM.

Next, we check if the current path contains a broken branch (Fig. 2.1a). We need to check for broken branches, because if we do not, the GAM will treat the last cylinder in the path to be a twig, which will unrealistically taper the broken branch, resulting in a volume underestimation of the broken branch. We define a broken branch as a first order branch with at most one second order branch attached to it. If the criteria are met, we set the minimum cylinder size of the path to be the last well fit first order branch cylinder. If there are not any well fit first order branch cylinders, the minimum cylinder branch size is 25% smaller than the last first order cylinder along the path.

Next, we fit a monotonic GAM to each path using the *cobs* R package (Ng & Maechler, 2007) and force the intercept of the model to be equal to our species-specific twig radius, or minimum cylinder radius in the case of broken branches. For the model parameters, we set *lambda* equal to 0.01, *degree* to 1, *constraint* to increase, and *nknots* to the number of good fit cylinders minus one. If there are ≤ 3 well fit cylinders in the path to model, we set the radius equal to the species-specific twig radius.

Finally, we combine the cylinders from all paths together, and take a weighed mean for each cylinder weighted by the cylinder radii. This is because the same cylinder can be in multiple paths. Optionally, we allow for modelling of the main stem as its own unique path without weighting the influence of the other paths, as the main stem is generally modeled well in QSMs, assuming that the main stem is roughly circular and does not contain large buttress flares (Arseniou et al., 2023; Demol et al., 2021b; Disney et al., 2018; Momo Takoudjou et al., 2018).

2.2.2 Calibration Data for Real Twig - Harvard Forest Trees

We selected five northern red oak (*Quercus rubra L.*) and five red maple (*Acer rubrum L.*) trees from a 2017 study in Harvard Forest (Petersham, MA, USA) to compare above ground woody biomass from destructive sampling with estimates of aboveground woody biomass from TLS-based approaches (Arseniou et al., 2023). The trees were healthy, covering a range of size classes and canopy positions. The ten trees were in two separate plots called the "main" and "north" plots, respectively, with the north plot located 30 meters NNE from the northeast corner of the main plot. The main plot was a 50 x 50 meter square delineated using a measuring tape and compass, with each edge aligned with the four main cardinal directions. The north plot was a 30 x 30 square delineated in the same way as the main plot. The ten trees were laser scanned in leaf-off conditions, and then destructively sampled in leaf-on conditions for detailed main stem mass, branch mass, and density measurements (Table 2.1).

Species	Tree	DBH (cm)	Height (m)	Main Stem Basic Density (g/cm^3)	Branch Basic Density (g/cm^3)	Main Stem Mass (kg)	Branch Mass (kg)	Total AGB (kg)
Acer rubrum	1	28.7	22.7	0.496	0.515	301.2	81.8	383.0
Acer rubrum	105	7.6	11.0	0.536	0.476	15.8	1.5	17.3
Acer rubrum	126	21.8	23.1	0.464	0.596	217.8	25.4	243.2
Acer rubrum	133	11.9	13.4	0.573	0.525	46.4	11.1	57.5
Acer rubrum	181	10.7	16.9	0.569	0.510	44.8	10.2	55.0
Quercus rubra	1	36.3	21.6	0.492	0.592	596.6	212.6	809.2
Quercus rubra	36	19.3	21.2	0.530	0.611	157.1	15.6	172.7
Quercus rubra	75	32.3	22.2	0.551	0.609	443.8	197.4	641.2
Quercus rubra	234	26.7	23.5	0.543	0.583	353.2	47.3	400.5
Quercus rubra	251	50.3	24.1	0.551	0.600	1103.8	313.5	1417.3

Table 2.1 Tree variables from destructively sampled trees from Harvard Forest in 2017. The main stem basic density is an average of the wood and bark density taken from multiple disks cut every four feet along the main stem. The branch basic density is an average of the wood and bark density taken from disks cut at the midpoint of all first order branches. All mass and density measurements are expressed on an oven dry basis.

2.2.3 Harvard Forest Terrestrial Laser Scanning & Data Processing

Each plot was systematically scanned with a Riegl VZ-400 (a time-of-flight sensor) in April 2017 during leaf-off conditions to minimize occlusion and maximize capture of the upper canopy branches. All scans were taken at a wavelength of 1550 nm, pulse rates of 100 or 300 kHz, and an angular resolution of 0.04 mrad, with multiple discrete returns and waveform output enabled. Given the sensor's beam divergence of 0.35 mrad, the spacing between individual points at 10 meters was approximately 6 millimeters. The main plot consisted of 48 scans total. 36 scans were taken inside the plot spaced 10 meters apart. Four additional scans were taken 25 meters from the plot edges along the four ordinal directions. The north plot consisted of 9 scans total. One scan was taken in the plot center. Four scans were taken 10 meters from the plot center in the four cardinal directions, while four scans were taken 21.2 meters from the plot center along the four ordinal directions. The individual scans from all plots were co-registered into a single point cloud using the Riegl RiSCAN PRO software with reference points being retroreflective targets placed in the field. The individual trees were extracted from the forest stand point cloud and down-sampled to a final resolution of 1.0 - 1.5 cm.

2.2.4 Harvard Forest Tree Measurements & Destructive Sampling

The ten trees were measured and destructively sampled in August 2017 during leaf-on conditions (Table 2.1). Diameter at breast height (DBH) was measured on each tree at 1.37 meters from the highest point on the ground with a diameter tape to the nearest 0.1 cm. After the trees were felled, the total tree height was measured from the base of the tree to the highest twig with a measuring tape. The trees were divided into the main stem and branch components, where the main stem progresses from the base of the tree and is the largest branch at each branching junction until the top of the tree is reached. The remaining parts of the tree were classified as branches. The mass of the main stem and branch components were immediately measured with a crane scale to capture their green mass. Disks were systematically cut along the main stem every four feet, and from the midpoint of every branch larger than 2.54 cm in diameter. The disks were immediately weighed to capture their green mass. The disks were peeled into wood and bark in the lab and then oven dried to estimate dry mass and basic density for the wood and bark. The basic density of each disk was calculated by averaging the basic density of the wood and bark. Finally, the basic density of the main stem and branches was calculated by averaging the basic densities of their corresponding disks. See Arseniou et al. (2023) for more details on the destructive sampling protocol. Table 2.1 summarizes the tree measurements.

2.2.5 Other Data for Additional Validation of Real Twig

To validate our Real Twig method outside of our training dataset, we opted to use publicly available datasets. These datasets were chosen to reflect how different processing workflows can affect the generation of QSMs of trees from TLS point clouds, given varying scanning conditions, point cloud quality, growing conditions, and tree size. The goal was to show that Real Twig could be applied to a variety of tree data sets, without *a priori* knowledge of destructive reference values.

The first dataset consists of 15 European ash (*Fraxinus excelsior L.*) trees, which were destructively sampled in 2017, in Belgium, with detailed green main stem density measurements, total green mass, total volume, and laser scanned in leaf off conditions with a Riegl VZ-1000 or VZ-400 scanner, which are both time-of-flight sensors (Demol et al., 2021a). These trees represent high-quality point clouds, laser scanned under near-optimal conditions, to test our Real Twig method. These trees represent a European even-aged management system, so tree variation and form were significantly impacted by management (Fig. 2.1b).

The second dataset consists of 12 Sessile oak (*Quercus petraea L.*) trees (Hackenberg et al., 2015b). These trees were laser scanned in 2013 during leaf off conditions in Germany with a Z+F IMAGER 5010c scanner, which is a phase-shift sensor. These trees were destructively sampled to get basic main stem density and total dry mass. These trees represent poor-form trees, with an abundance of epicormic sprouts, growing in a natural stand (Fig. 2.1, c, d, e). The trees were also scanned under poor weather conditions, so the point clouds were observed to be affected by wind and rain noise. These trees represent lower-quality point clouds, with quality destructive sampling reference data, to test our Real Twig method. We did not use the already filtered point clouds in our analysis, but instead used the raw plot data, and manually segmented and filtered the twelve trees using CloudCompare (CloudCompare, 2023). We down-sampled the final point clouds to a resolution of 1.0 cm.

The last dataset consisted of four large, old-growth, tropical trees from Brazil, which were laser scanned with a Riegl VZ-400 (a time-of-flight sensor) in 2018 (Burt et al., 2021). Since these trees are tropical trees from Brazil, they could only be scanned in leaf on conditions. The leaves were virtually removed from the point cloud using the TLSeparation algorithm (Vicari et al., 2019). The trees were also destructively sampled with detailed volumes, total dry mass, and basic main stem density values. This dataset represents high-quality point clouds and reference data for very large trees, with the added uncertainty of leaf removal, to test our Real Twig method.

Tree measurement data for the public data sets are shown in Table 2.2.

Dataset	Species	Tree	DBH (cm)	Height (m)	Main Stem Density (g/cm^3)	Total AGB (kg)
Burt et al. (2021)	*Inga alba*	1	64.7	29.8	0.568	3960.1
Burt et al. (2021)	*Hymenaea courbaril*	2	117.9	46.2	0.769	18584.2
Burt et al. (2021)	*Tachigali paniculata*	3	90.5	34.9	0.639	8392.6
Burt et al. (2021)	*Trattinnickia burserifolia*	4	69.7	35.2	0.567	5521.1
Demol et al. (2021)	*Fraxinus excelsior*	1	27.4	21.7	0.841[a]	705.5[a]
Demol et al. (2021)	*Fraxinus excelsior*	2	22.6	20.6	0.839[a]	416.1[a]
Demol et al. (2021)	*Fraxinus excelsior*	3	19.4	18.4	0.805[a]	239.7[a]
Demol et al. (2021)	*Fraxinus excelsior*	4	20.4	21.0	0.761[a]	266.0[a]
Demol et al. (2021)	*Fraxinus excelsior*	5	11.5	12.6	0.814[a]	61.9[a]
Demol et al. (2021)	*Fraxinus excelsior*	6	30.9	18.3	0.815[a]	543.0[a]
Demol et al. (2021)	*Fraxinus excelsior*	7	12.4	13.2	0.808[a]	77.1[a]
Demol et al. (2021)	*Fraxinus excelsior*	8	28.6	21.5	0.797[a]	789.6[a]
Demol et al. (2021)	*Fraxinus excelsior*	9	19.7	21.1	0.851[a]	300.1[a]
Demol et al. (2021)	*Fraxinus excelsior*	10	12.6	13.0	0.760[a]	61.5[a]
Demol et al. (2021)	*Fraxinus excelsior*	11	25.8	20.3	0.890[a]	474.0[a]
Demol et al. (2021)	*Fraxinus excelsior*	13	35.3	19.0	0.907[a]	904.0[a]
Demol et al. (2021)	*Fraxinus excelsior*	14	39.8	22.5	0.896[a]	1444.0[a]
Demol et al. (2021)	*Fraxinus excelsior*	15	33.7	20.1	0.824[a]	905.9[a]
Demol et al. (2021)	*Fraxinus excelsior*	16	22.6	18.2	0.800[a]	406.0[a]
Hackenberg et al. (2015)	*Quercus petraea*	1	24.5	25.5	0.530	458.8
Hackenberg et al. (2015)	*Quercus petraea*	2	24.2	26.6	0.520	311.0
Hackenberg et al. (2015)	*Quercus petraea*	3	31.7	29.0	0.520	595.3
Hackenberg et al. (2015)	*Quercus petraea*	4	26.3	28.6	0.540	517.6
Hackenberg et al. (2015)	*Quercus petraea*	5	28.7	24.8	0.530	412.2
Hackenberg et al. (2015)	*Quercus petraea*	6	27.5	29.4	0.510	468.7
Hackenberg et al. (2015)	*Quercus petraea*	7	24.0	27.2	0.520	366.1
Hackenberg et al. (2015)	*Quercus petraea*	8	30.0	27.6	0.510	632.9
Hackenberg et al. (2015)	*Quercus petraea*	9	29.2	31.1	0.520	581.8
Hackenberg et al. (2015)	*Quercus petraea*	10	27.1	22.7	0.520	411.8
Hackenberg et al. (2015)	*Quercus petraea*	11	25.7	25.8	0.510	452.2
Hackenberg et al. (2015)	*Quercus petraea*	12	29.4	27.3	0.530	589.6

Table 2.2 Tree variables from publicly available datasets. Each dataset represents different growing conditions and point cloud quality to test our Real Twig method. Main stem basic density and AGB are on a dry mass basis, except for those trees indicated with [a] which are on a green mass basis. All density values are an average of multiple disks collected along the main stem.

2.2.6 Twig Measurements

Our search of the literature revealed that measurements of tree twig diameters are not common. So, we selected trees of varied sizes and ages of the appropriate species, planted on the Michigan State University campus and measured twig diameters using a Pittsburg 6” Dial Caliper (Model #92437). We measured one to four unique twigs on each tree in perpendicular directions depending on the accessibility of the twigs from the ground. We randomly chose the starting azimuth of the first twig by multiplying the second hand of a watch by sixty to convert it into an azimuth. We used a Suunto MC-2 hand compass to find the starting azimuth and ensure the measurements were perpendicular to each other. We measured the diameter of the twig to the nearest hundredth of an inch at the midpoint of the twig, between the current year’s growth and the previous year’s terminal bud scar, being careful to avoid any swelling from lateral buds. Finally, we averaged the twig diameters, converted diameters to radii by dividing the diameters in half, and converted the units from inches to millimeters.

Sessile oak has not been planted on Michigan State University’s campus and is not naturalized in Michigan, USA. To test our method on the Sessile oak trees from the publicly available dataset by Hackenberg et al. (2015b), we used twig measurements from another publicly available dataset from the Altitudinal Vicariants dataset collected in northern Spain (Milla & Reich, 2011), accessed from the TRY plant trait database (Kattge et al., 2020). Milla and Reich measured their twig diameters to the nearest hundredth of a millimeter at the base of the twig. We also used the Bridge dataset (Baraloto et al., 2010), available from the TRY plant trait database (Kattge et al., 2020), containing stem and leaf traits from French Guiana for the four large tropical trees (Burt et al., 2021), which were also not present on Michigan State University’s campus.

Dataset	Species	n	Mean	Min	Max	SD	CV
This Study	*Acer rubrum*	30	1.18	0.89	1.52	0.16	0.14
This Study	*Fraxinus americana*	30	2.45	1.78	3.68	0.34	0.14
This Study	*Fraxinus pennsylvanica*	30	2.33	1.52	2.79	0.28	0.12
This Study	*Fraxinus quadrangulata*	30	2.77	2.16	4.44	0.54	0.2
This Study	*Fraxinus spp.*	90	2.51	1.52	4.44	0.39	0.15
This Study	*Quercus rubra*	30	1.47	0.89	2.41	0.33	0.23
Milla & Reich	*Quercus petraea*	10	1.90	1.35	2.45	0.37	0.19
Baraloto et al.	*Hymenaea courbaril*	1	6.81	6.81	6.81	-	-
Baraloto et al.	*Inga alba*	2	5.79	3.47	8.11	3.28	0.57
Baraloto et al.	*Tachigali paniculata*	2	6.93	5.91	7.95	1.44	0.21
Baraloto et al.	*Trattinnickia spp.*	1	5.80	5.80	5.80	-	-

Table 2.3 Twig radii measurements in millimeters (mm).

2.2.7 Non-Destructive Volume Estimation

For the Harvard data, we generated QSMs for the 10 trees using two versions of TreeQSM (v2.4.1 and v2.3.0). We used two different versions of TreeQSM to ensure our method training was not overfit to a single version of TreeQSM or individual QSMs. We also wanted to compare the drastic volume differences we observed between different versions of TreeQSM and understand its cause. For the other data sets, we used only the latest version of TreeQSM (v2.4.1 at the time of writing) for validating our Real Twig method, as new users are most likely to download the latest version.

We started by generating 40 unique QSMs for each tree using unique combinations of input parameters with the *define_inputs* function from TreeQSM v2.4.1. We generated two values for *PatchDiam1*, 10 values for *PatchDiam2Min*, and two values for *PatchDiam2Max*. We chose to generate 10 values for *PatchDiam2Min*, as it has the greatest impact on small branch reconstruction during the cylinder fitting process (Demol et al., 2022b). TreeQSM's input combinations are multiplicative, giving us a total of 40 unique input parameter combinations. From the 40 models, we chose the optimal input parameters with a custom metric. For our custom metric, we maximized the *SurfCov* parameter (the percentage of the cylinder's surface covered by points) and minimized the *mad* parameter (the mean absolute distance from the cylinder's surface to the underlying points).

Using the optimal input parameters, we generated 30 additional QSMs using both TreeQSM v2.3.0 and v2.4.1 to account for underlying stochasticity inherent to QSM generation (Calders et al., 2015b; Disney et al., 2018), and volume differences between the two versions. From the 30 new models with the optimal input parameters, we chose the optimal model that had the lowest *mad* which is the default behavior for TreeQSM. For all the QSMs generated, we enabled the parabolic branch tapering and parent child corrections, which are the default settings for TreeQSM. TreeQSM returns both the original, unmodified cylinder data, and the modified cylinder data, so we did not need to generate additional QSMs to test our Real Twig method, since Real Twig works on the unmodified cylinder data. For the European ash trees, we followed the same procedure as the Harvard data using TreeQSM 2.4.1.

For the Sessile oak and large tropical trees, we wanted to test our Real Twig method for different use cases of TreeQSM (v2.4.1) without any a priori knowledge about the measured mass and volumes of the trees. For our QSM input parameters, we used the *define_inputs* function to automatically select a single best *PatchDiam1*, *PatchDiam2Min*, and *PatchDiam2Max*. Using these parameters, we generated thirty QSMs to account for any stochasticity in QSM generation and had TreeQSM automatically select the best model with the lowest mad. We left all other input parameters as the defaults to best represent a typical use case of TreeQSM.

For the large tropical trees, we opted to use TreeQSM's (v2.4.1) triangulation mesh for estimating the volume of the main stem up until the first branch. These trees contained large buttress flares which TreeQSM was unable to properly reconstruct, leading to oversized cylinders, with circular diameters the width of the buttress. We could have manually removed the buttress flares from the point cloud as was done by Burt et al. (2021), however we found a triangulation mesh better captures the main stem volume and has proven effective for estimating the total mass of tropical trees in similar studies (Momo Takoudjou et al., 2018).

2.2.8 Comparisons of Biomass and Volume Outputs from TreeQSM and Real Twig

TreeQSM returns volume estimates for both the main stem and branch components. Our analyses of the training data showed that the best, currently available correction for incorrectly sized cylinders is the local taper correction method of Raumonen et al. (2013) described in the introduction. We wanted to compare the Real Twig method of correcting QSMs to the best, currently available approach, using independent reference data.

The best reference data we had in each data set were total tree biomass estimates, with separate branch and stem biomass estimates available for the Harvard Forest trees. Since we had tree density measurements and mass estimates from the destructive sampling, we compared differences in biomass generated by different versions of TreeQSM with and without the Real Twig method employed against reference destructive sampling data. Since all biomass estimates were generated by multiplying QSM volume by the same tree's density estimates, the only differences in biomass were due to differences in the volume estimates from the QSMs.

We chose to use the Harvard trees to train our Real Twig method because of the detailed stem and branch density values, which allowed us to convert the QSM branch and stem volumes into aboveground biomass by multiplying the individual volume components (main stem and branch volumes) by their corresponding basic density values from destructive sampling. We needed to calculate separate stem and branch masses to ensure there were not any compensating errors in total biomass estimates that masked the effectiveness of using Real Twig for correcting branch mass and volume overestimation in QSMs. The total mass was the sum of the mass of a tree's branches and its main stem.

None of the public datasets had separate branch density values, so we were only able to assess the accuracy of total mass and were unable to check for any compensating errors between the main stem and branches. For the Demol et al. (2021a) European ash trees, only green density was taken from disks along the main stem, so only total green biomass could be compared. All other calculations were on a dry mass basis, as were the mass validation metrics described in the next section. See Table 2 for a summary of the public datasets used in this analysis.

2.2.9 Statistical Analysis

We calculated the following standard validation metrics for each dataset (Arseniou et al., 2023; Burt et al., 2021; Calders et al., 2015b) comparing different TLS-based mass estimates to the reference destructive data.

Individual tree error:

$$\mathcal{E} = \text{Mass}_{\text{TLS}} - \text{Mass}_{\text{Ref}}$$

Individual tree relative error:

$$\text{RE} = \frac{|\mathcal{E}|}{\text{Mass}_{\text{Ref}}}$$

Mean relative error (%) across all trees:

$$\text{MRE\%} = \frac{1}{n}\sum_{i=1}^{n} \text{RE}_i \times 100\%$$

Root mean square error across all trees:

$$\text{RMSE} = \sqrt{\frac{1}{n}\sum_{i=1}^{n} \mathcal{E}_i^2}$$

Relative root mean square error (%) across all trees:

$$\text{RMSE\%} = \frac{\text{RMSE}}{\text{Mean\_Mass}_{\text{Ref}}} \times 100\%$$

In the above equations, $Mass_{TLS}$ is the TLS mass estimate of a single tree by converting QSM volume to mass with the tree's unique density values. $Mass_{TLS}$ will be either, total, stem, or branch mass depending on if the dataset has branch specific density values for a tree. $Mass_{Ref}$ is the reference mass from destructive sampling. It will either be the tree's corresponding total, stem, or branch mass depending on the dataset. *i* refers to a single tree, while *n* refers to all trees in the dataset. $Mean\_Mass_{Ref}$ is the mean mass for either the total, stem, or branch mass in the dataset. Finally, we quantified the difference between the $Mass_{TLS}$ and $Mass_{Ref}$ using the concordance correlation coefficient (CCC) (Lin, 1989). All statistical analyses, tables, and figures were created using R (R Core Team, 2023).

2.3 Results

2.3.1 Comparisons of Real Twig and Different TreeQSM Versions for the Harvard Trees

All methods used to generate volumes and masses from the Harvard trees were precise and accurate for modeling the main stems of the trees, with CCC values close to 1, though there was a general bias towards overestimating main stem biomass by 15-30% for stems < 150 kg. For both versions of TreeQSM, main stem biomass estimates were close to the reference main stem mass, with a RMSE% of 7.0% and a CCC of 0.997 for v2.3.0, while v2.4.1 had a RMSE% of 6.7% and a CCC of 0.998 (Table 2.4). With Real Twig, the main stem biomass estimates were similar to TreeQSM, with a RMSE% of 6.9% and a CCC of 0.997 with Real Twig applied to v2.3.0, and a RMSE% of 7.2% and a CCC of 0.997 with Real Twig applied to v2.4.1. For v2.4.1, Real Twig slightly reduced the MRE% of the main stem biomass and slightly increased the RMSE% across the ten trees, with the opposite pattern being true when Real Twig was applied to v2.3.0.

For the branch biomass of the Harvard Forest trees, there were significant differences between all methods. TreeQSM v2.3.0 performed better than v2.4.1, with v2.4.1 at least doubling mass estimation errors for all statistics (Table 2.4). TreeQSM v2.3.0 overestimated branch biomass with an MRE% of 363%, a RMSE% of 160%, and a CCC value of 0.654. TreeQSM v2.4.1 severely overestimated branch biomass with an MRE% of 949%, a RMSE% of 346%, and a CCC value of 0.381. In contrast, Real Twig with TreeQSM v2.4.1 had highly accurate branch biomass estimates, with an MRE% of -0.7%, a RMSE% of 8.4%, and a CCC value of 0.997. Real Twig with TreeQSM v2.3.0 showed as modest underestimation of branch biomass, with an MRE% of -9.1%, a RMSE% of 16.5%, and a CCC value of 0.989. Overall, Real Twig dramatically improved branch biomass estimates when compared to the current, best-available corrections in either version of TreeQSM, reducing the average error in total AGB estimates by three orders of magnitude for v2.4.1 and with a thirty-six-fold reduction in error for v2.3.0.

For the total biomass, the total error is the sum of the main stem and branch components. The results show that errors in the total mass estimates are mostly the result of branch biomass overestimation (Fig. 2.2). TreeQSM v2.4.1 had the largest overestimation, with an MRE% of

126%, a RMSE% of 77.6%, and a CCC value of 0.831. TreeQSM v2.3.0 overestimated the total mass less, with an MRE% of 50%, a RMSE% of 37.2%, and a CCC value of 0.947. Real Twig applied to TreeQSM v2.4.1 performed the best, with an MRE% of 0.02%, a RMSE% of 6.7%, and a CCC value of 0.998. Real Twig applied to TreeQSM v2.3.0 also performed very well with an MRE% of 2.2%, a RMSE% of 5.7%, and a CCC value of 0.998. Overall, Real Twig dramatically improved total biomass estimates compared to the current, best-available corrections in either version of TreeQSM, dropping the average error total AGB estimates by two orders of magnitude for v2.4.1 and with a twenty-five-fold reduction in error for v2.3.0.

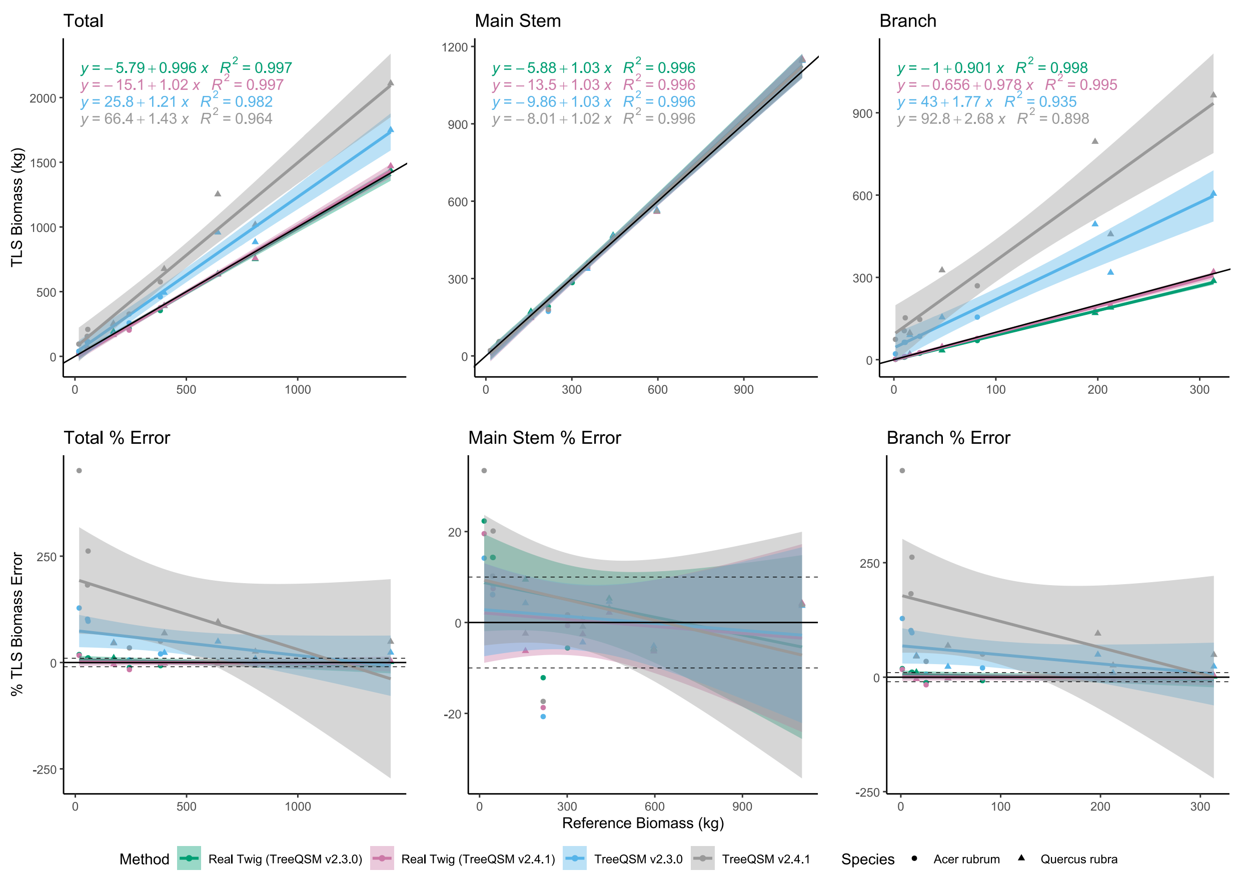

Figure 2.2 Mass estimates for the Harvard Forest trees using two different versions of TreeQSM with and without Real Twig. The horizontal dashed lines are the ± 10% error lines. The solid black line is the identity line.

TreeQSM v2.4.1				TreeQSM v2.3.0			
Metric	Total AGB	Main Stem Biomass	Branch Biomass	Metric	Total AGB	Main Stem Biomass	Branch Biomass
Mean Relative Error (%)	126.428	4.581	949.317	Mean Relative Error (%)	50.529	1.204	363.772
RMSE (kg)	325.973	22.217	317.471	RMSE (kg)	156.127	23.138	146.843
Relative RMSE (%)	77.672	6.773	346.454	Relative RMSE (%)	37.202	7.053	160.249
CCC	0.831	0.998	0.381	CCC	0.947	0.997	0.654
Real Twig (TreeQSM v2.4.1)				**Real Twig (TreeQSM v2.3.0)**			
Metric	Total AGB	Main Stem Biomass	Branch Biomass	Metric	Total AGB	Main Stem Biomass	Branch Biomass
Mean Relative Error (%)	0.019	0.493	-0.691	Mean Relative Error (%)	2.198	4.700	-9.095
RMSE (kg)	27.187	23.653	7.736	RMSE (kg)	24.101	22.747	15.081
Relative RMSE (%)	6.478	7.210	8.442	Relative RMSE (%)	5.743	6.934	16.457
CCC	0.998	0.997	0.997	CCC	0.998	0.997	0.989

Table 2.4 Accuracy statistics for the Harvard Forest trees broken down into total, main stem, and branch components.

2.3.2 Validation of Real Twig with European Ash Trees

For the twelve European ash trees studied (Fig. 2.3), Real Twig dramatically increased the accuracy and precision of the total green mass estimates, with only one tree falling outside ± 10% of the reference mass (Fig. 2.3). TreeQSM v2.4.1 overestimated total mass by 60.8% on average, with a RMSE% of 107% and a CCC of 0.645 (Table 2.5), while Real Twig showed very high accuracy in total mass (MRE = 0.2%), with a RMSE% of 6.3% and a CCC of 0.996.

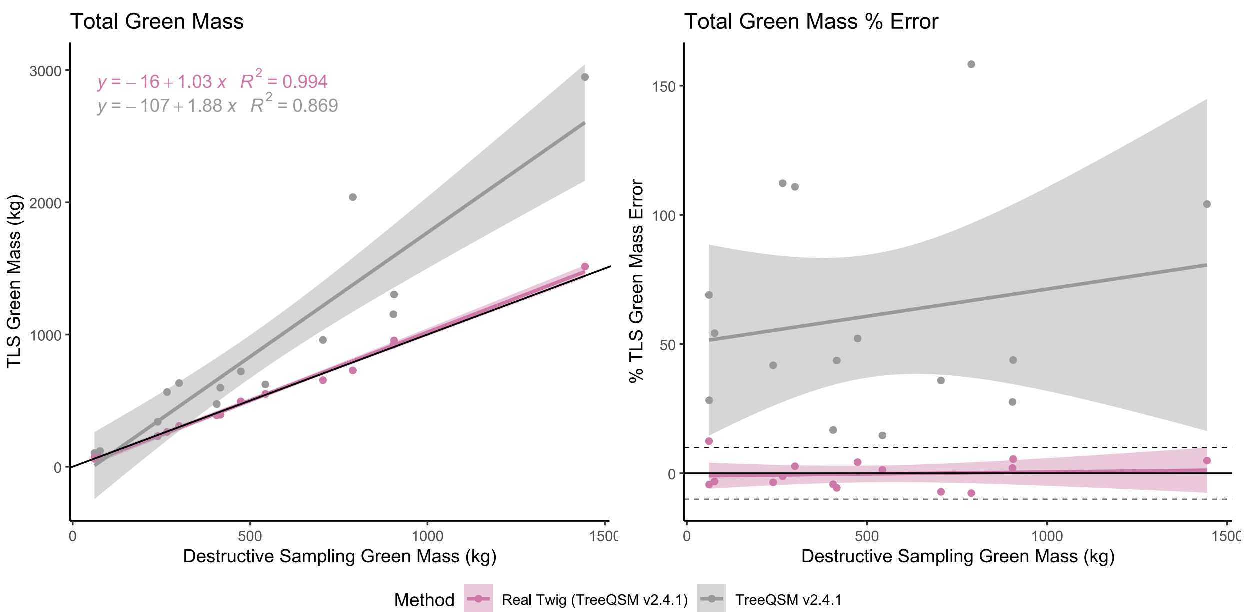

Figure 2.3 Sixteen European ash trees with mass estimates from TreeQSM and Real Twig. The horizontal dashed lines are the ± 10% error lines. The solid black line is the identity line.

Method	Mean Relative Error (%)	RMSE (kg)	Relative RMSE (%)	CCC
Real Twig (TreeQSM v2.4.1)	-0.268	32.236	6.367	0.996
TreeQSM v2.4.1	60.877	543.207	107.291	0.645

Table 2.5 Accuracy statistics for the European ash trees.

2.3.3 Validation of Real Twig for Sessile Oak Trees

Compared to the Harvard and European ash trees, the Real Twig results were far less precise for the Sessile oak trees, with a CCC value of 0.897. However, the Real Twig results were still drastically more accurate than TreeQSM v2.4.1, with the latter having a CCC value of only 0.173. Real Twig was able to improve the accuracy of nearly all the trees, with most of them falling within ± 10% of the reference mass after correction (Fig. 2.4). TreeQSM had an MRE of 74.7% on average, with a RMSE of 78.7%, while Real Twig had an MRE of -1.5% on average, with an RMSE of 9.2% (Table 2.6). Both TreeQSM and Real Twig were unbiased, with little correlation between mass overestimation and tree size, over the size range of these trees.

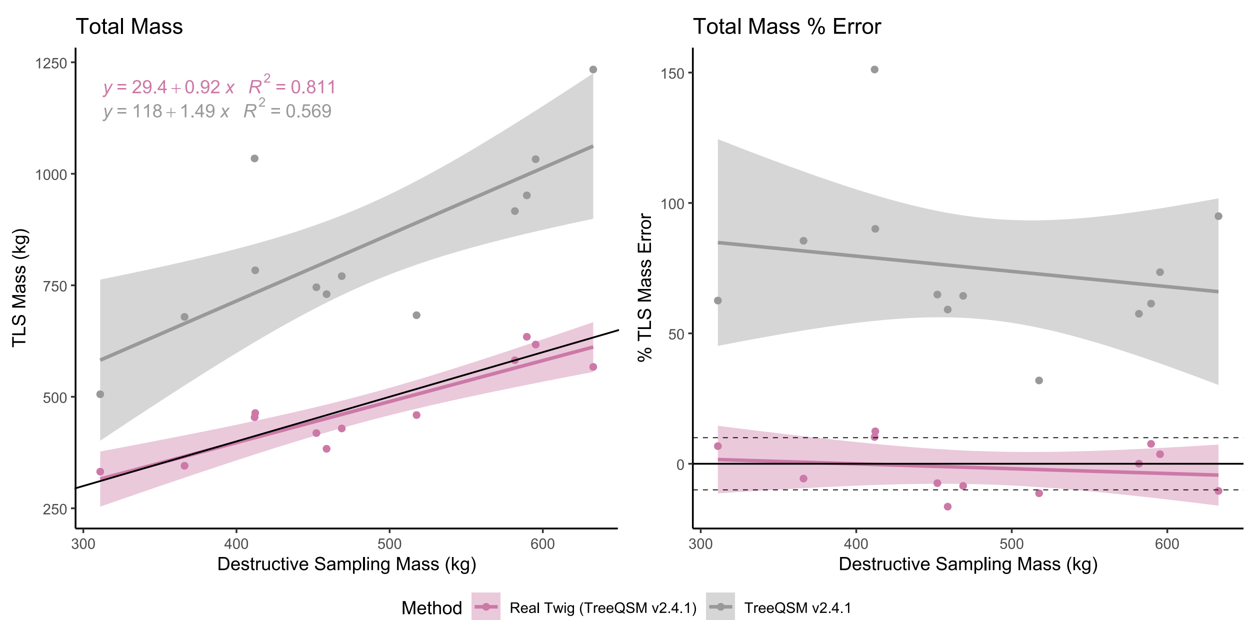

Figure 2.4 Twelve Sessile oak trees with mass estimates from TreeQSM and Real Twig. The horizontal dashed lines are the ± 10% error lines. The solid black line is the identity line.

Method	Mean Relative Error (%)	RMSE (kg)	Relative RMSE (%)	CCC
Real Twig (TreeQSM v2.4.1)	-1.576	44.687	9.249	0.897
TreeQSM v2.4.1	74.753	380.232	78.696	0.173

Table 2.6 Accuracy statistics for the Sessile oak trees.

2.3.4 Validation of Real Twig for Large Tropical Trees

The large tropical trees showed an overall error difference between TreeQSM and Real Twig that was lower than that seen for the other data sets (Fig. 2.5). In both cases, the total mass estimates are roughly parallel to the reference line, but TreeQSM v2.4.1 generally overestimated total mass, while Real Twig generally underestimated the total mass, with MRE% values of 18% and -6.5%, respectively (Table 2.7). For TreeQSM, the RMSE% and CCC values are 17 and 0.973, respectively, while Real Twig has RMSE% and CCC values of 4.7 and 0.998, respectively. However, Real Twig increased the precision of the total mass estimates, with an absolute bias reduced by three-fold compared to the current, best-available correction for TreeQSM (Fig. 2.5 & Table 2.7).

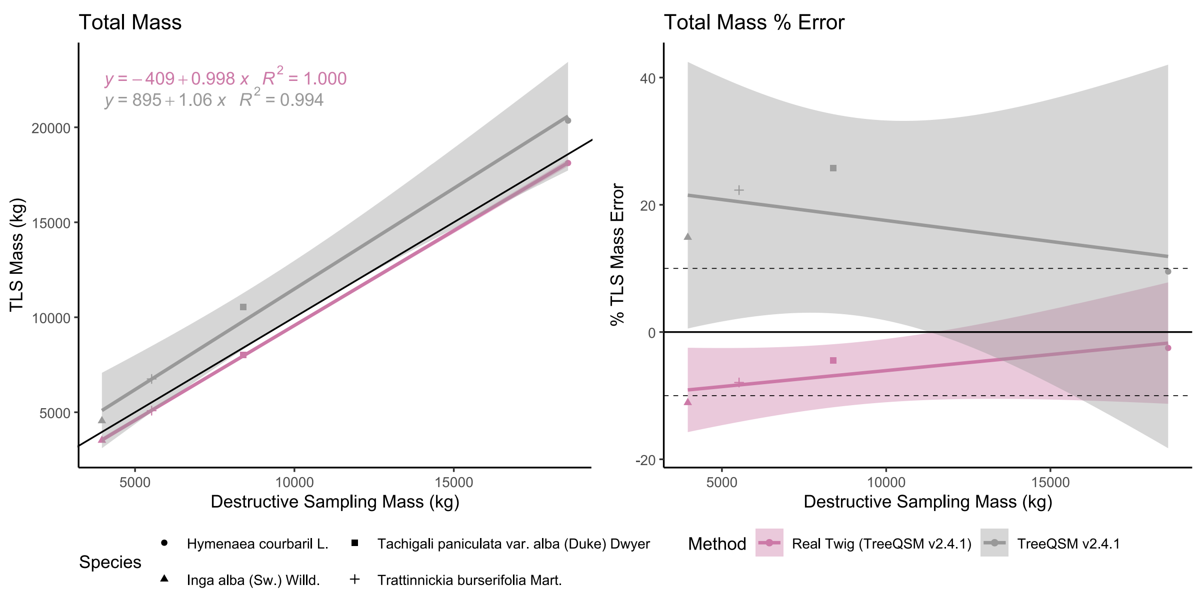

Figure 2.5 Four large tropical trees with mass estimates from TreeQSM and Real Twig. The horizontal dashed lines are the ± 10% error lines. The solid black line is the identity line.

Method	Mean Relative Error (%)	RMSE (kg)	Relative RMSE (%)	CCC
Real Twig (TreeQSM v2.4.1)	-6.505	430.915	4.728	0.998
TreeQSM v2.4.1	18.114	1554.169	17.052	0.973

Table 2.7 Accuracy statistics for the large tropical trees.

2.3.5 Overall Performance of Real Twig for All Study Trees

When all the study trees are combined, Real Twig greatly outperforms TreeQSM v2.4.1, the current best algorithm. TreeQSM consistently overestimates total mass over a wide range of tree sizes, while Real Twig showed highly accurate mass estimates (Table 2.8, Fig. 2.6). For TreeQSM, the RMSE% and CCC values were 48.7% and 0.982, respectively, while Real Twig had RMSE% and CCC values of 10.5% and 0.999, respectively. Looking at all trees together (Figure 2.6), we can see that Real Twig's error correction exponentially decreases compared to TreeQSM v2.4.1 as the size of the trees increases, because there is a smaller proportion of total mass in small branches. One of the smallest trees in the study had a %MRE of greater than 400%, which was corrected to a little over 10% error with the Real Twig method (Fig. 2.6). On the other hand, all the study trees had %MRE >10% when not corrected with the Real Twig method.

Method	Mean Relative Error (%)	RMSE (kg)	Relative RMSE (%)	CCC
Real Twig (TreeQSM v2.4.1)	-1.190	138.783	10.528	0.999
TreeQSM v2.4.1	76.754	641.746	48.683	0.982

Table 2.8 Accuracy statistics across all trees in the study.

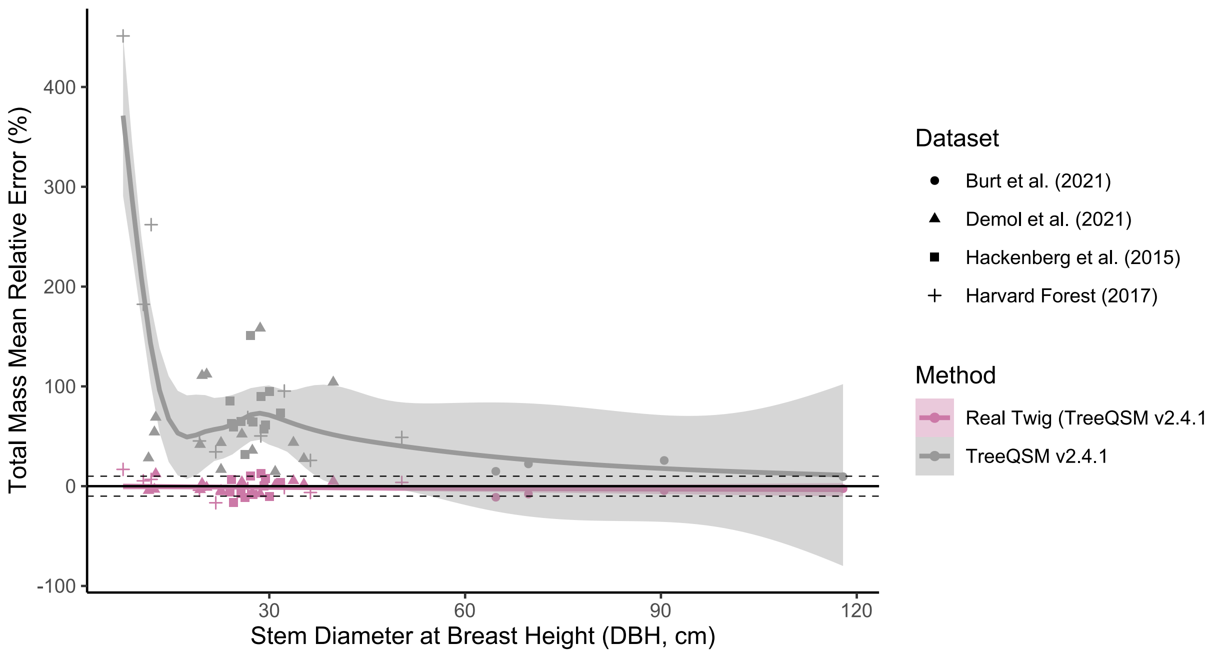

Figure 2.6 Mean relative error (%) of total aboveground biomass estimated from QSM-generated volumes, using two different approaches, applied to trees of different size (stem diameter at breast height, DBH, cm) from different data sets (symbols).

2.4 Discussion

2.4.1 Improved Tree Volume and Biomass Estimation from QSMs with Real Twig

TLS has emerged as a legitimate, non-destructive way to estimate total tree above ground woody biomass or volume with a reasonable degree of precision and accuracy, as many studies have now demonstrated (Arseniou et al., 2023; Calders et al., 2015b; Demol et al., 2022a; Gonzalez de Tanago et al., 2018; Lau et al., 2019; Momo Takoudjou et al., 2018). However, Demol et al. (2022b) recently cautioned that significant volume overestimations will likely be a problem until advances in understanding of laser scanning best practices, data processing, and QSM software can solve the problem of overestimation of smaller portions of the tree (i.e., small branches and twigs). This study shows that the Real Twig method can greatly improve the precision and accuracy of tree volume and biomass estimation, by dramatically improving the volume estimates of smaller portions of trees modeled with a QSM, in this case TreeQSM. Out of the 41 trees of different species, obtained from the multiple, independent data sets examined, every tree showed a large increase in mass accuracy and precision, with most falling within our target goal of ± 10% of the reference mass and total mass errors as low as 0.04%. By contrast, the current version of TreeQSM (v2.4.1) with the most advanced cylinder fitting and segmentation routine always produced mass estimates greater than 10% of the reference values from destructive sampling, with some small trees exceeding > 400% overestimation.

The Real Twig method was successful because it improves upon previous approaches to deal with the small branch overestimation issue. We were not satisfied with the practice of not attempting to model smaller parts of the tree, by discarding branches below a given diameter threshold. Our results show that this could only be a viable solution when trees are very large (Fig. 2.6) and smaller branches and twigs are not a significant component of total mass and is an incomplete solution in any event. Such an approach also does not allow for estimating the volume or mass of smaller trees, composed of smaller parts. Since planting new trees is a significant strategy within forest carbon offset projects that help remove carbon dioxide from the atmosphere to mitigate climate change (Nilsson & Schopfhauser, 1995; Pacala & Socolow, 2004), it is important to be able to estimate the change in tree biomass over time for younger, faster-growing trees (McMahon et al., 2010; Yang et al., 2023).

A major improvement with Real Twig is the rescaling of every cylinder in the tree by incorporating ideas from the local tapering approach of Raumonen et al. (2013) and the existence of a whole-tree allometry from Hackenberg et al. (2015a). While Real Twig does not assume that every part of a tree has the same allometry, it remodels different parts of the tree to be realistic, by modeling every path in the tree and averaging across paths, allowing local corrections in the allometry of individual parts of the tree to be connected to the architecture of the whole tree.

Another major innovation was recognizing that it is not only possible, but likely, that none of the cylinders in the smaller parts of a tree will be correctly modeled by the QSM. The allometric modeling approach of Hackenberg et al. (2015a) uses the whole population of cylinders to fit an allometric model to determine outliers and correct them. But, if the QSM data does not contain many correctly modeled small cylinders, then coefficients of the model fit to the raw data will be biased, specifically toward overestimation of small parts of the tree. Our solution was to measure actual twig diameters for the species of interest, or to use published values, to force the taper model to taper to the appropriate twig size and rescale the taper of each branch path to be realistic.

2.4.2 Differences in Volume Estimation Between Different Versions of TreeQSM

There were large differences in the two versions of TreeQSM software used to generate tree volume (and mass) estimates in this study, with and without the Real Twig correction. This is the first study to show such large version differences, and an important finding, because the same data could produce very different estimates of tree volume and biomass. This would be particularly problematic if changes in forest volume or biomass over time were computed with different versions of the software. It is also notable that the difference between the different versions of TreeQSM is reduced when the Real Twig correction method is applied. Examining these differences helped us to better understand the results of the study and potential improvements to TreeQSM, other QSM methods, and Real Twig.

Our analysis suggests that TreeQSM has evolved toward an improved ability to reconstruct branches and correctly represent the tree's topology in later versions, with the consequence of exacerbating the small branch overestimation problem inherent to the input point cloud (Fig. 2.7). The oldest version of TreeQSM (v2.0) does not successfully reconstruct the higher order branches of the input point cloud and has visible issues with branch topology, leading to branch volume omission. Version 2.3.x improves the branching topology and reconstructs more, higher-order branches, leading to a more realistic QSM, and therefore more branch volume. Finally, version 2.4.x reconstructs even more higher order branches and improves on the tree topology, but has a more relaxed taper constraint, leading to a substantial increase in high order branch volume.

TreeQSM version 2.4.x overestimates total tree volume because it fits better to the input point cloud, finding more branches and providing a more realistic topology of the tree, at the expense of including point cloud related errors, such as beam divergence, wind noise, and co-registration errors, while older versions (2.0 – 2.3.x) omit branches and have a strictly enforced taper, regardless of the underlying point cloud data, leading to volume omission (Pasi Raumonen, personal communication, June 13, 2023). This explains why post-processing tree point clouds after the initial registration can reduce QSM volume overestimation when wind and occlusion errors are not factors (Demo et al., 2022b; Wilkes et al., 2021). Additionally, TreeQSM v2.3.x reconstructs fewer branches than v2.4.x, and the branches that are reconstructed are around 10% shorter than v2.4.x (Pasi Raumonen, personal communication, June 13, 2023). This means that earlier versions of TreeQSM could have produced seemingly more accurate estimates of tree volume and biomass, due to compensating errors (i.e., omitting small branches that are actually present in the real tree), while overestimating the volume of smaller branches that are included. Because the smaller twigs are missing, the path lengths are reduced, and smaller branches abruptly end before reaching actual twigs, but are modeled as twigs in the QSM. This is a likely explanation for the significant (-9%) average underestimation of branch biomass when Real Twig was applied to TreeQSM v2.3.x (Table 2.3). This is also a likely explanation of the results of previous validation studies using older versions of TreeQSM, with an overestimation bias of 9.68% to 21% (Calders et al., 2015b; Demol et al., 2021b) compared to more recent studies that found tree volumes more than doubled in their overestimation at 52%, with most of the error occurring in the small branches when using TreeQSM v2.4.x (Demol et al., 2022b).

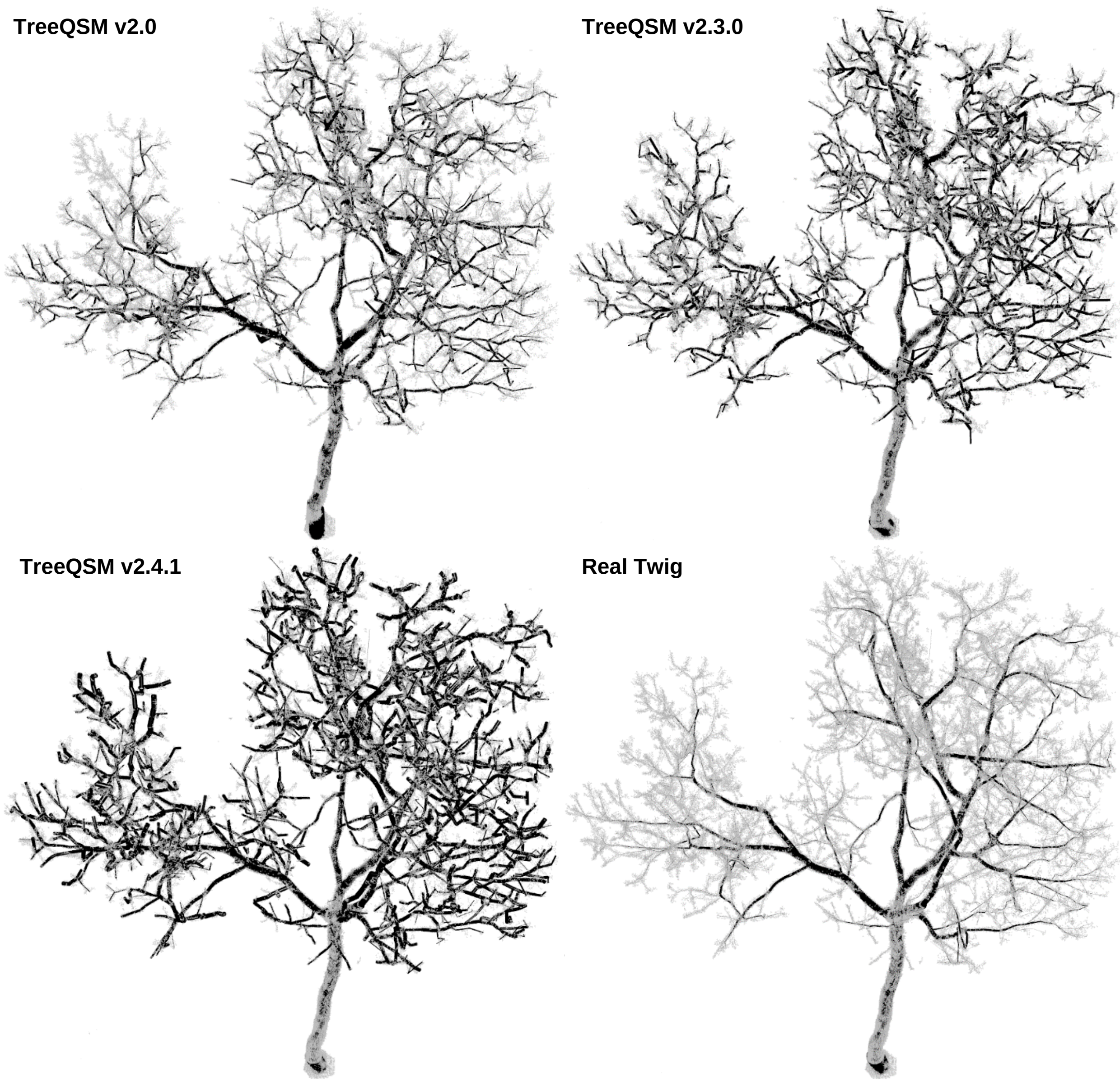

Figure 2.7 Top-down view of a northern red oak from Harvard Forest showing the difference in tapering, topology, branch connectivity, and cylinder radii between different versions of TreeQSM and Real Twig. The QSM cylinders colored in black are overlaid on top of the input point cloud colored in light gray. All QSMs have the same input parameters as possible between the different versions and have the same input point cloud. The Real Twig QSM uses the raw cylinder fits from the v2.4.1 show here.

2.4.3 Implications of Size-Dependent Error in Tree Volume and Biomass Estimation with QSM Based Approaches

Our results clearly show that the relative error in AGB estimated from QSMs can be very high for small trees, which are composed of only small parts, without the Real Twig correction. We also showed that this error declines asymptotically toward smaller and smaller estimation errors, when applied to trees of increasing size (Fig. 2.6). By contrast, (Calders et al., 2015b) reported that error in AGB estimates from QSMs were independent of DBH. We suspect that our results differ from theirs because they examined error over a more limited size range of trees from about 10 to 65 cm DBH, whereas we included much smaller and much larger trees. Other studies validating TLS with destructive sampling reference also show that for larger trees (>1500 kg) TLS mass is closer to the reference destructive mass, and vice versa for smaller trees (<1500 kg) (Burt et al., 2021; Calders et al., 2015b; Demol et al., 2021b; Demol et al., 2022b; Hackenberg et al., 2015b; Momo Takoudjou et al., 2018). We believe the source of this pattern lies in the proportion of twigs and small branches in a tree. The larger the tree's total volume, the less twig volume contributes to total tree volume. In contrast, the smaller the tree's total volume, the more twigs and small branches contribute to the total tree volume.

Twig size also plays a role, as the smaller the actual twig diameter, the harder it is for TLS to accurately resolve, leading to oversized twigs in point clouds and QSMs. In the case of large tropical trees, most of their mass is in the main stem and large branches, while their twigs are stout with diameters approaching 1 cm (Table 2.3). This is an ideal situation for TLS, where most twigs can be captured, and their volume contributes little to the total tree volume. This explains the pattern in our own results, where total mass overestimation systematically decreases as total mass increases (Fig. 2.6).

This issue of size-dependence in the success of AGB estimation with TLS and QSMs has important implications for choosing how to obtain data for building allometric equations to predict AGB from DBH. Databases of destructive sampling measurements of AGB are often missing large trees (Weiskittel et al., 2015) because of the difficulty in finding, or justifying the felling of, very large trees. Our results show that the best case for obtaining good estimates with QSM-based estimation approaches may be for large trees. By contrast, it is very easy and cost efficient to destructively sample small trees, which represent the worst-case scenario for QSM-based estimation approaches. Our results show that carbon sequestration could be drastically overestimated if QSM-based approaches were employed without correction with a method such as Real Twig. In general, QSM-based solutions for estimating mass of volume of small trees and small parts of trees need more scrutiny.

2.4.4 Considerations for Improved Tree Volume and Biomass Estimation from QSMs

Our Real Twig method can correct QSM volume overestimation in small branches and twigs, resulting in dramatic increases in accuracy of branch and total tree volume and mass estimation from TLS-QSM-based approaches. For the best total tree volume estimates, we recommend starting with the highest possible quality point cloud. 'Quality' is a subjective term, but for this purpose, we refer to quality as the best topological representation of the tree with minimal occlusion and a well-defined woody skeleton. We recommend, if possible, using point clouds in the "leaf-off" condition to achieve this. Burt et al. (2021) showed that removing the leaves from a "leaf-on" point cloud is a necessity for accurate AGB estimates, otherwise AGB will be overestimated upwards of 40%. This is because leaves can be included in what are modeled as twigs in the point cloud, magnifying the overestimation error.

Our results showed a lower level of accuracy improvements from Real Twig for large tropical trees, which could have been the result of removing leaf points from point clouds (these were the only trees we examined that were scanned in a 'leaf-on' condition). Arseniou et al. (2021a) showed that artificial leaf removal from point clouds with the TLSeparation algorithm (Vicari et al., 2019) can result in the accidental removal of twigs and small, higher-order branches. So, it is possible that some of the underestimation of total tropical tree biomass by Real Twig came from assuming that the twigs were slightly larger parent branches, because the actual twigs were removed by the leaf removal algorithm. This error could be even larger if Real Twig is applied to QSMs constructed from point clouds of smaller trees with their leaf points removed. To minimize this problem, we recommend using Real Twig with TreeQSM v2.4.1, as it reconstructs more high-order branch cylinders from the point cloud, and when corrected with Real Twig, gives the most realistic models of the trees (see Figs. 2.2 & 2.6). We also recommend visually inspecting each optimal QSM against its input point cloud to ensure the QSM with the best topology is selected.

It is important to understand that Real Twig was trained only with realistic twig diameter measurements and not with actual measurements along the main stem and branches of the trees. As a result, what our method determines to be a good or bad cylinder fit may occasionally exclude correctly modeled cylinders, especially in smaller diameter branches, which could lead to overaggressive tapering in smaller parts of the tree. Our method could also artificially increase the diameter of branch bases, especially if the branch base cylinder was determined to be a poor fit. This is a side effect of using growth length as the radius predictor variable in the GAM, as every time there is a fork in a tree, the growth length of a cylinder decreases. Without enough well-fit cylinders with similar growth lengths, the GAM predicts the radius based on the closest well-fit cylinders, which could inflate the branch base, and decrease the smaller branches, as the closest well-fit cylinder for small branches is the measured twig diameter. This could create a path that is inflated at the path base and too narrow as growth length decreases. These small errors could cancel out and still yield accurate branch volumes, but at the expense of correctness of path tapering relative to the real tree. As a general principle, the best total tree volume estimates will have QSMs that are visually close to the actual tree, with the input parameters determined either visually or automatically (Calders et al., 2015a). Regarding input parameters, we recommend using a semi-automated approach, where the starting input parameters are chosen automatically, before being manually reduced gradually, until the maximum amount of small branch detail is achieved while still maintaining proper topology.

Another consideration is the accuracy and generality of tree density estimates, which convert QSM volumes to tree mass. While we were able to generate precise and accurate estimates of total tree mass with only main stem density values from the public datasets, we had the lowest total mass estimate error when we used tree-specific main stem and branch densities (i.e., the Harvard data). Using separate tree-specific main stem and branch densities is important for the accurate conversion of volume to woody mass, because there can be a large density variation within a tree between its main stem and branch components (Demol et al., 2021a; Disney et al., 2018; MacFarlane, 2020). If the main stem and branch density are not equal, using the incorrect density for either may lead to systematic bias when converting to total tree mass even if the total tree volume from the QSM is correct. Another little-discussed issue is bark density, as TLS scans the tree's outside bark volume, and bark differs in density from wood and occupies a variable portion of total tree volume (Neumann & Lawes, 2021). Future validation studies should consider how to accurately separate wood and bark components of volume or both branches and stem and include detailed measurements of both wood and bark density of stems and branches.

Finally, our results show that Real Twig can overcome well known deficiencies in both time-of-flight and phase-shift sensor technologies and their ability to resolve fine details in trees, such as beam divergence and co-registration errors. However, the end goal is not merely to correct known errors, but to better understand the errors inherent to specific TLS sensors and mitigate them as much as possible in the field, by matching the appropriate sensor and parameters to the trees being scanned. While studies have investigated some of these sensor deficiencies and their effect on QSMs, they do so with only one sensor and fixed sets of input parameters (Morhart et al., 2024; Wilkes et al., 2021). Future studies should consider multiple laser scanning sensor technologies, with varying input parameters, such as the effect of angular resolution and distance or scan numbers, on trees in situ and controlled environments, relating the results back to the species' measured twig diameter, and Real Twig's ability to overcome these deficiencies. Until TLS sensor technology can resolve these fine details efficiently and accurately, Real Twig or similar corrections must serve as the final step in the data processing pipeline to ensure precise and accurate metrics from QSMs.

2.5 Conclusion

We see three next steps for further calibration and validation of the Real Twig method. First, more intelligent cylinder radii and broken branch filters need to be developed. The filters should identify good and bad fit cylinders based on their taper within the QSM itself, their growth length or relative position in the tree or path, and their relationship to the measured twig diameter. The filter should be dynamic, retaining more small cylinders for higher quality QSMs, and fewer small cylinders for lesser quality QSMs. Identifying correctly modeled cylinders will allow for better modeling between different tree growth forms, especially excurrent growth forms that retain multiple broken lower branches. Future work will focus on testing Real Twig for a broader range of species and tree architectures, especially excurrent growth forms, such as those for pines, which have whorls of branches attached to a dominant main stem, and more abrupt tapering along paths. Here, we only look at tree species with a deliquescent branching architecture.

Second, the method relies on having measured twig diameters for a specific tree species. While reviewing the literature of this paper and searching for already published data sets, we were surprised how few studies of trees and forests have included measurements of tree twigs. Thus, the twig measurements published here add much needed data to fill this data gap. Collaboration in the research community is needed to measure more twig diameters across different countries and tree species. While our results show a genus-average twig diameter is a reasonable substitute for a specific species' twig diameter, if the genus average is not available, or the species is unknown, the twig diameter will be uncertain. Given the time it takes to measure a few twigs on a tree, we recommend tree-specific measurements on every tree scanned, unless time or cost prohibitive. These measurements will not only improve the accessibility of Real Twig but will also provide valuable reference data for future tree modeling using remote sensing data.

Finally, work is underway to allow Real Twig to be updated to support other QSM modeling programs to help make accurate and precise tree volume estimates more accessible to the remote sensing community. The Real Twig method currently supports the cylinder-based approaches of TreeQSM (Raumonen et al., 2013) and SimpleForest (Hackenberg et al., 2014), but the method can be implemented for any geometric primitive based approach that provides information on parent-child relationships.

REFERENCES

Åkerblom, M., Raumonen, P., Mäkipää, R., & Kaasalainen, M. (2017). Automatic tree species recognition with quantitative structure models. Remote Sensing of Environment, 191, 1–12. https://doi.org/10.1016/j.rse.2016.12.002

Arseniou, G., MacFarlane, D. W., Calders, K., & Baker, M. (2023). Accuracy differences in aboveground woody biomass estimation with terrestrial laser scanning for trees in urban and rural forests and different leaf conditions. Trees - Structure and Function. https://doi.org/10.1007/s00468-022-02382-1

Arseniou, G., MacFarlane, D. W., & Seidel, D. (2021a). Measuring the Contribution of Leaves to the Structural Complexity of Urban Tree Crowns with Terrestrial Laser Scanning. Remote Sensing, 13(14), 2773. https://doi.org/10.3390/rs13142773

Arseniou, G., MacFarlane, D. W., & Seidel, D. (2021b). Woody Surface Area Measurements with Terrestrial Laser Scanning Relate to the Anatomical and Structural Complexity of Urban Trees. Remote Sensing, 13(16), 3153. https://doi.org/10.3390/rs13163153

Baraloto, C., Paine, C. E. T., Poorter, L., Beauchene, J., Bonal, D., Domenach, A. M., Hérault, B., Patiño, S., Roggy, J. C., & Chave, J. (2010). Decoupled leaf and stem economics in rain forest trees. Ecology Letters, 13(11), 1338–1347. https://doi.org/10.1111/J.1461-0248.2010.01517.X

Burt, A., Boni Vicari, M., Da Costa, A. C. L., Coughlin, I., Meir, P., Rowland, L., & Disney, M. (2021). New insights into large tropical tree mass and structure from direct harvest and terrestrial lidar. Royal Society Open Science, 8(2), 201458. https://doi.org/10.1098/rsos.201458

Calders, K., Adams, J., Armston, J., Bartholomeus, H., Bauwens, S., Bentley, L. P., Chave, J., Danson, F. M., Demol, M., Disney, M., Gaulton, R., Krishna Moorthy, S. M., Levick, S. R., Saarinen, N., Schaaf, C., Stovall, A., Terryn, L., Wilkes, P., & Verbeeck, H. (2020). Terrestrial laser scanning in forest ecology: Expanding the horizon. Remote Sensing of Environment, 251. https://doi.org/10.1016/J.RSE.2020.112102

Calders, K., Burt, A., Newnham, G., Disney, M., Murphy, S., Raumonen, P., Herold, M., Culvenor, D., Armston, J., Avitabile, V., & Kaasalainen, M. (2015). Reducing uncertainties in above-ground biomass estimates using terrestrial laser scanning. Proceedings of Silvilaser, 197–199.

Calders, K., Newnham, G., Burt, A., Murphy, S., Raumonen, P., Herold, M., Culvenor, D., Avitabile, V., Disney, M., Armston, J., & Kaasalainen, M. (2015). Nondestructive estimates of above-ground biomass using terrestrial laser scanning. Methods in Ecology and Evolution, 198–208. https://doi.org/10.1111/2041-210X.12301

Calders, K., Origo, N., Burt, A., Disney, M., Nightingale, J., Raumonen, P., Åkerblom, M., Malhi, Y., & Lewis, P. (2018). Realistic Forest Stand Reconstruction from Terrestrial LiDAR for Radiative Transfer Modelling. Remote Sensing, 10(6), 933. https://doi.org/10.3390/rs10060933

Calders, K., Verbeeck, H., Burt, A., Origo, N., Nightingale, J., Malhi, Y., Wilkes, P., Raumonen, P., Bunce, R. G. H., & Disney, M. (2022). Laser scanning reveals potential underestimation of biomass carbon in temperate forest. Ecological Solutions and Evidence, 3(4). https://doi.org/10.1002/2688-8319.12197

CloudCompare (2.11.3). https://www.danielgm.net/cc/.

Csárdi, G., Nepusz, T., Horvát, S., Traag, V., Zanini, F., & Noom, D. (2023). igraph. Zenodo. https://doi.org/10.5281/zenodo.7573267

Demol, M., Calders, K., Krishna Moorthy, S. M., Van den Bulcke, J., Verbeeck, H., & Gielen, B. (2021). Consequences of vertical basic wood density variation on the estimation of aboveground biomass with terrestrial laser scanning. Trees, 35(2), 671–684. https://doi.org/10.1007/s00468-020-02067-7

Demol, M., Calders, K., Verbeeck, H., & Gielen, B. (2021). Forest above-ground volume assessments with terrestrial laser scanning: a ground-truth validation experiment in temperate, managed forests. Annals of Botany, 128(6), 805–819. https://doi.org/10.1093/aob/mcab110

Demol, M., Verbeeck, H., Gielen, B., Armston, J., Burt, A., Disney, M., Duncanson, L., Hackenberg, J., Kükenbrink, D., Lau, A., Ploton, P., Sewdien, A., Stovall, A., Momo Takoudjou, S., Volkova, L., Weston, C., Wortel, V., Calders, K., & Alberto Silva, C. (2022). Estimating forest above-ground biomass with terrestrial laser scanning: Current status and future directions. Methods Ecol Evol, 13, 1628–1639. https://doi.org/10.1111/2041-210X.13906

Demol, M., Wilkes, P., Raumonen, P., Krishna Moorthy, S., Calders, K., Gielen, B., & Verbeeck, H. (2022). Volumetric overestimation of small branches in 3D reconstructions of & Fraxinus excelsior; Silva Fennica, 56(1). https://doi.org/10.14214/sf.10550

Disney, M. I., Boni Vicari, M., Burt, A., Calders, K., Lewis, S. L., Raumonen, P., & Wilkes, P. (2018). Weighing trees with lasers: Advances, challenges and opportunities. Interface Focus, 8(2). https://doi.org/10.1098/rsfs.2017.0048

Fan, G., Nan, L., Dong, Y., Su, X., & Chen, F. (2020). AdQSM: A New Method for Estimating Above-Ground Biomass from TLS Point Clouds. Remote Sensing, 12(18), 3089. https://doi.org/10.3390/rs12183089

Frank, J., Weiskittel, A., Walker, D., Westfall, J. A., Radtke, P. J., Affleck, D. L. R., Coulston, J., & MacFarlane, D. W. (2019). Gaps in available data for modeling tree biomass in the United States. https://doi.org/10.2737/NRS-GTR-184

Gonzalez de Tanago, J., Lau, A., Bartholomeus, H., Herold, M., Avitabile, V., Raumonen, P., Martius, C., Goodman, R. C., Disney, M., Manuri, S., Burt, A., & Calders, K. (2018). Estimation of above-ground biomass of large tropical trees with terrestrial LiDAR. Methods in Ecology and Evolution, 9(2), 223–234. https://doi.org/10.1111/2041-210X.12904

Hackenberg, J., & Bontemps, J.-D. (2023). Improving quantitative structure models with filters based on allometric scaling theory. Applied Geomatics, 15(4), 1019–1029. https://doi.org/10.1007/s12518-023-00537-4

Hackenberg, J., Morhart, C., Sheppard, J., Spiecker, H., & Disney, M. (2014). Highly Accurate Tree Models Derived from Terrestrial Laser Scan Data: A Method Description. 5, 1069–1105. https://doi.org/10.3390/f5051069

Hackenberg, J., Spiecker, H., Calders, K., Disney, M., Raumonen, P., Hyyppä, J., Liang, X., & Puttonen, E. (2015). SimpleTree-An Efficient Open Source Tool to Build Tree Models from TLS Clouds. 6, 4245–4294. https://doi.org/10.3390/f6114245

Hackenberg, J., Wassenberg, M., Spiecker, H., & Sun, D. (2015). Non Destructive Method for Biomass Prediction Combining TLS Derived Tree Volume and Wood Density. 6, 1274–1300. https://doi.org/10.3390/f6041274

Holopainen, M., Vastaranta, M., Kankare, V., Räty, M., Vaaja, M., Liang, X., Yu, X., Hyyppä, J., Hyyppä, H., Viitala, R., & Kaasalainen, S. (2012). BIOMASS ESTIMATION OF INDIVIDUAL TREES USING STEM AND CROWN DIAMETER TLS MEASUREMENTS. The International Archives of the Photogrammetry, Remote Sensing and Spatial Information Sciences, XXXVIII-5/W12, 91–95. https://doi.org/10.5194/isprsarchives-XXXVIII-5-W12-91-2011

Houghton, R. A. (2005). Aboveground Forest Biomass and the Global Carbon Balance. Global Change Biology, 11(6), 945–958. https://doi.org/10.1111/j.1365-2486.2005.00955.x

Kattge, J., Bönisch, G., Díaz, S., Lavorel, S., Prentice, I. C., Leadley, P., Tautenhahn, S., Werner, G. D. A., Aakala, T., Abedi, M., Acosta, A. T. R., Adamidis, G. C., Adamson, K., Aiba, M., Albert, C. H., Alcántara, J. M., Alcázar C, C., Aleixo, I., Ali, H., … Wirth, C. (2020). TRY plant trait database – enhanced coverage and open access. Global Change Biology, 26(1), 119–188. https://doi.org/10.1111/gcb.14904

Lau, A., Calders, K., Bartholomeus, H., Martius, C., Raumonen, P., Herold, M., Vicari, M., Sukhdeo, H., Singh, J., & Goodman, R. (2019). Tree Biomass Equations from Terrestrial LiDAR: A Case Study in Guyana. Forests, 10(6), 527. https://doi.org/10.3390/f10060527

Liang, X., Kankare, V., Hyyppä, J., Wang, Y., Kukko, A., Haggrén, H., Yu, X., Kaartinen, H., Jaakkola, A., Guan, F., Holopainen, M., & Vastaranta, M. (2016). Terrestrial laser scanning in forest inventories. ISPRS Journal of Photogrammetry and Remote Sensing, 115, 63–77. https://doi.org/10.1016/j.isprsjprs.2016.01.006

Lin, L. I.-K. (1989). A Concordance Correlation Coefficient to Evaluate Reproducibility. Biometrics, 45(1), 255. https://doi.org/10.2307/2532051

MacFarlane, D. W. (2020). Functional Relationships Between Branch and Stem Wood Density for Temperate Tree Species in North America. Frontiers in Forests and Global Change, 3. https://doi.org/10.3389/ffgc.2020.00063

MacFarlane, D. W., Kuyah, S., Mulia, R., Dietz, J., Muthuri, C., & Van Noordwijk, M. (2014). Evaluating a non-destructive method for calibrating tree biomass equations derived from tree branching architecture. Trees, 807–817. https://doi.org/10.1007/s00468-014-0993-2

McMahon, S. M., Parker, G. G., & Miller, D. R. (2010). Evidence for a recent increase in forest growth. Proceedings of the National Academy of Sciences, 107(8), 3611–3615. https://doi.org/10.1073/pnas.0912376107

Milla, R., & Reich, P. B. (2011). Multi-trait interactions, not phylogeny, fine-tune leaf size reduction with increasing altitude. Annals of Botany, 107, 455–465. https://doi.org/10.1093/aob/mcq261

Momo Takoudjou, S., Ploton, P., Sonké, B., Hackenberg, J., Griffon, S., de Coligny, F., Guy Kamdem, N., Libalah, M., II Mofack, G., Le Moguédec, G., Pélissier, R., & Barbier, N. (2018). Using terrestrial laser scanning data to estimate large tropical trees biomass and calibrate allometric models: A comparison with traditional destructive approach. Methods of Ecolology and Evolution, 9, 905–916. https://doi.org/10.1111/2041-210X.12933

Montès, N., Gauquelin, T., Badri, W., Bertaudière, V., & Zaoui, E. H. (2000). A non-destructive method for estimating above-ground forest biomass in threatened woodlands. Forest Ecology and Management, 130(1–3), 37–46. https://doi.org/10.1016/S0378-1127(99)00188-7

Morhart, C., Schindler, Z., Frey, J., Sheppard, J. P., Calders, K., Disney, M., Morsdorf, F., Raumonen, P., & Seifert, T. (2024). Limitations of estimating branch volume from terrestrial laser scanning. *European Journal of Forest Research*, *143*(2), 687–702. https://doi.org/10.1007/s10342-023-01651-z

Neumann, M., & Lawes, M. J. (2021). Quantifying carbon in tree bark: The importance of bark morphology and tree size. Methods in Ecology and Evolution, 12(4), 646–654. https://doi.org/10.1111/2041-210X.13546

Ng, P., & Maechler, M. (2007). A Fast and Efficient Implementation of Qualitatively Constrained Quantile Smoothing Splines. Statistical Modelling, 7(4), 315–328. https://doi.org/10.1177/1471082X0700700403

Nilsson, S., & Schopfhauser, W. (1995). The carbon-sequestration potential of a global afforestation program. Climatic Change, 30(3), 267–293. https://doi.org/10.1007/BF01091928

Pacala, S., & Socolow, R. (2004). Stabilization Wedges: Solving the Climate Problem for the Next 50 Years with Current Technologies. Science, 305(5686), 968–972. https://doi.org/10.1126/science.1100103

R Core Team. (2023). R: A Language and Environment for Statistical Computing. https://www.R-project.org/

Raumonen, P., Kaasalainen, M., Akerblom, M., Kaasalainen, S., Kaartinen, H., Vastaranta, M., Holopainen, M., Disney, M., & Lewis, P. (2013). Remote Sensing Fast Automatic Precision Tree Models from Terrestrial Laser Scanner Data. Remote Sens, 5, 491–520. https://doi.org/10.3390/rs5020491

Stovall, A. E. L., Vorster, A. G., Anderson, R. S., Evangelista, P. H., & Shugart, H. H. (2017). Non-destructive aboveground biomass estimation of coniferous trees using terrestrial LiDAR. Remote Sensing of Environment, 200, 31–42. https://doi.org/10.1016/j.rse.2017.08.013

Terryn, L., Calders, K., Disney, M., Origo, N., Malhi, Y., Newnham, G., Raumonen, P., Åkerblom, M., & Verbeeck, H. (2020). Tree species classification using structural features derived from terrestrial laser scanning. ISPRS Journal of Photogrammetry and Remote Sensing, 168, 170–181. https://doi.org/10.1016/j.isprsjprs.2020.08.009

Vicari, M. B., Disney, M., Wilkes, P., Burt, A., Calders, K., & Woodgate, W. (2019). Leaf and wood classification framework for terrestrial LiDAR point clouds. Methods in Ecology and Evolution, 10(5), 680–694. https://doi.org/10.1111/2041-210X.13144

Vorster, A. G., Evangelista, P. H., Stovall, A. E. L., & Ex, S. (2020). Variability and uncertainty in forest biomass estimates from the tree to landscape scale: the role of allometric equations. Carbon Balance and Management, 15(1), 8. https://doi.org/10.1186/s13021-020-00143-6

Weiskittel, A. R., MacFarlane, D. W., Radtke, P. J., Affleck, D. L. R., Temesgen, H., Woodall, C. W., Westfall, J. A., & Coulston, J. W. (2015). A Call to Improve Methods for Estimating Tree Biomass for Regional and National Assessments. Journal of Forestry, 113(4), 414–424. https://doi.org/10.5849/jof.14-091

Wilkes, P., Lau, A., Disney, M., Calders, K., Burt, A., Gonzalez de Tanago, J., Bartholomeus, H., Brede, B., & Herold, M. (2017). Data acquisition considerations for Terrestrial Laser Scanning of forest plots. Remote Sensing of Environment, 196, 140–153. https://doi.org/10.1016/j.rse.2017.04.030

Wilkes, P., Shenkin, A., Disney, M., Malhi, Y., Bentley, L. P., & Vicari, M. B. (2021). Terrestrial laser scanning to reconstruct branch architecture from harvested branches. Methods in Ecology and Evolution, 12(12), 2487–2500. https://doi.org/10.1111/2041-210X.13709

Yang, H., Ciais, P., Frappart, F., Li, X., Brandt, M., Fensholt, R., Fan, L., Saatchi, S., Besnard, S., Deng, Z., Bowring, S., & Wigneron, J.-P. (2023). Global increase in biomass carbon stock dominated by growth of northern young forests over past decade. Nature Geoscience, 16(10), 886–892. https://doi.org/10.1038/s41561-023-01274-4

Yang, W., Wilkes, P., Vicari, M. B., Hand, K., Calders, K., & Disney, M. (2024). Treegraph: Tree Architecture from Terrestrial Laser Scanning Point Clouds. *Remote Sensing in Ecology and Conservation*. https://doi.org/10.1002/rse2.399

CHAPTER 3

RTWIG: AN R PACKAGE TO CORRECT OVERESTIMATED SMALL BRANCHES AND TWIGS IN QUANTITATIVE STRUCTURE MODELS OF TREES

Abstract

Quantitative structure models (QSM) provide detailed topological cylinder models of trees, built off point clouds of trees. QSMs allow for efficient estimation of total tree volume without the need for destructively sampled reference measurements. QSMs also measure aspects of trees that were traditionally impossible to measure (such as total tree surface area). However, QSM modeling software severely overestimates the volume of small branches and twigs due to technological limitations of current laser scanning sensors. Here, we present an R package, *rTwig*, to correct branch volume overestimation in QSMs with the Real Twig method. We also include a novel database of twig diameter measurements for a wide range of tree genera and species. *rTwig* creates QSMs with realistic branch tapering, constrained by the species' actual twig measurement, and generates accurate tree volume estimates. *rTwig* also contains a collection of tools for QSM manipulation and visualization seamlessly compatible with the R ecosystem.

3.1 Introduction

Over the past decade, terrestrial laser scanning (TLS) has become an efficient method to estimate total tree volume non-destructively (Arseniou et al., 2023; Calders et al., 2015; Demol et al., 2022a; Disney et al., 2018; Holopainen et al., 2012; Stovall et al., 2017). Using TLS, trees are captured as a point cloud, three-dimensional coordinates in space co-registered from multiple scan locations into a local coordinate system, measuring parts of trees at a specific point in time that are difficult or impossible to capture without harvesting the tree (Calders et al., 2020). Technical biases and limitations inherent to different laser scanning sensors are well documented, making TLS less susceptible to human measurement error compared to traditional ground-based measurements, by representing the tree holistically with millions of unique data points (Calders et al., 2018, 2020). TLS now allows for previously impossible-to-obtain measurements, such as the surface area of all branches (Arseniou et al., 2021).

However, TLS struggles to accurately resolve small branches and twigs < 5-7 cm in diameter in a tree, due to the following limitations in current TLS sensors (Abegg et al., 2017; Demol et al., 2022b; Disney et al., 2018; Wilkes et al., 2017, 2021):

1. Beam exit diameter and divergence: the widening of the initial laser beam footprint with increasing distance from the sensor.

2. Occlusion: anterior objects preventing the laser pulse from hitting posterior objects, creating gaps in the final point cloud.

3. Wind: the movement of branches and twigs creating misalignment between parts of the tree as they sway back and forth.

4. Co-registration errors: the inability of registration software to perfectly align multiple scans.

From the point cloud, total tree volume can be estimated with quantitative structure models (QSM), which fit cylinders to the point cloud to represent the tree's topology (Fan et al., 2020; Hackenberg et al., 2015a; Raumonen et al., 2013), from which tree-specific structural metrics, such as total volume, can be easily extracted from the topologically connected network of cylinders (Åkerblom et al., 2017; Arseniou et al., 2021; Terryn et al., 2020).

Once the total volume of a tree is known from its QSM, above ground biomass (AGB) can be estimated non-destructively by multiplying the QSM volume by measured or published wood density values (Arseniou et al., 2023). QSM stem and branch volumes can then be compared to reference measurements to evaluate their accuracy for biomass modeling. While QSMs can show good agreement with their reference destructive sampling data (Arseniou et al., 2023; Burt et al., 2021; Calders et al., 2015; Demol et al., 2021b; Momo Takoudjou et al., 2018), the volume estimates from QSMs are limited by their input point cloud data. Current QSM software programs reconstruct cylinders from the point cloud directly, including all the point cloud issues, often doubling the volume of twigs and small branch cylinders (Demol et al., 2021a; Demol et al., 2022b; Hackenberg et al., 2015b; Wilkes et al., 2021).

There are three distinct methods to reduce volume overestimation in QSMs. The first method is to remove all branches with a base cylinder diameter ≤ 5-7 cm and only model the larger parts of the tree (Demol et al., 2021a; Gonzalez de Tanago et al., 2018). Omitting all the small branches is not suitable for extracting whole-tree metrics. The next method is an allometric correction. In this method, a mathematical function is fit to all QSM cylinders using an independent predictor variable; cylinder radii that fall outside a defined confidence interval are assumed to be overestimated and are resized to the predicted value (Hackenberg et al., 2015a; Hackenberg & Bontemps, 2023). This approach reduces volume overestimation but assumes the allometry of the tree is always identical in all parts of the tree. If parts of the tree deviate from this fixed allometry, cylinder radii are dramatically increased or decreased, which does not reflect the real taper within the tree. The final method employed by Raumonen et al. (2013) and Wilkes et al. (2021) uses individual branch cylinder radii to adjust the taper of each branch by constraining cylinders in each branch to be smaller than those in their parent branches, combined with a parabolic model forcing the branch to taper towards a fixed minimum constraint. This approach is data driven and logical assuming a perfect input point cloud, but it can resize cylinder radii that do not need correction and inflate the radii of small branches and twigs.

To overcome the small branch overestimation problem in QSMs, we developed *rTwig*, a software package built for the R environment (R Core Team, 2024). *rTwig* corrects every overestimated cylinder in a QSM using the method we call “Real Twig”. Real Twig identifies every path in a QSM, from the base of the main stem to each twig tip and fits a general additive taper model to every path in the tree's QSM path network. Real Twig realistically constrains the model by tapering each path to end in a twig the size of measured twig diameters for a given species. A novel data base of twig diameter measurements for common North American tree genera and species is also included in the package to make these measurements immediately accessible to the user. The result is a QSM that is visually realistic, has precise estimates of total tree volume for all parts of the tree, and retains the tree's proper allometry. *rTwig* is optimized for all major platforms (Windows, MacOS, and Linux) and supports popular QSM software packages, including TreeQSM (Raumonen et al., 2013) and SimpleForest (Hackenberg et al., 2015a).

3.2 Methods

3.2.1 Software Design

We designed *rTwig* to be compatible with both base R (R Core Team, 2024) and popular data analysis packages such as the *Tidyverse* (Wickham et al., 2019). Due to non-linear scaling of file size and computation costs needed to process QSMs of different sized trees, *rTwig* was written with efficiency and performance in mind. All *rTwig* functions are written using base R or with the *tidytable* package (Fairbanks, 2024), which provides *Tidyverse* syntax with the performance gains of the *data.table* package (Barrett et al., 2024). Importing a QSM made with TreeQSM in MATLAB (MathWorks, 2022) is done with the *rmatio* (Widgren & Hulbert, 2023) and *R.matlab* (Bengtsson, 2022) packages. QSM path analysis is done with the *igraph* package (Csárdi et al., 2023). Efficient general additive modeling (GAM) is carried out using the *cobs* package (Ng & Maechler, 2022). Parallel processing is handled by the *future* package (Bengtsson, 2021). By default, multisession parallel backend is used for all platforms, but efficient multicore forking is also available for MacOS and Linux systems. Point cloud and QSM cylinder visualization is implemented with the *rgl* package (Murdoch & Adler, 2024). Finally, QSM mesh exporting is done with the *Morpho* (Schlager, 2017) package.

3.2.2 Real Twig Method

Real Twig was designed to deal with the small branch radii overestimation problem in QSMs. Real Twig is distinct from traditional QSM branch tapering methods by using parts of a QSM that are well modeled, such as large branches, and using them to improve poorly modeled parts, such as small branches and twigs (see example in Fig. 3.1). Real Twig models every path in a QSM. A path starts at the base of the tree and ends at a twig, with the total number of paths being equal to the number of twigs in the QSM. Real Twig fits a monotonic generalized additive model (GAM) to cylinders along the path, incorporating species-specific twig measurements (described in the next section) and existing path allometry to correct the poorly modeled portions of the QSM (Fig. 3.1, a & d). The method forces the paths to end in a realistically sized twig and models the rest of the branch path behind it to taper branches realistically (Fig. 3.1, c & f). A detailed description of the Real Twig method can be found in Morales & MacFarlane (2024).

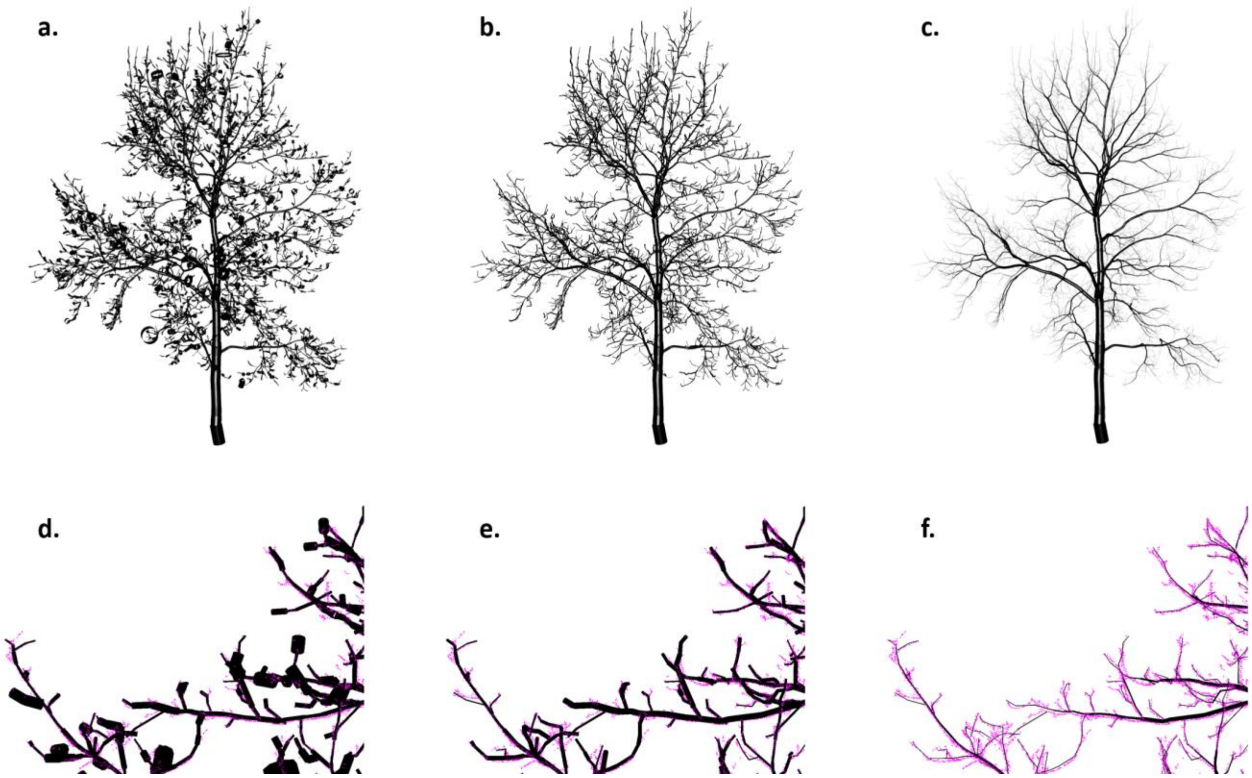

Figure 3.1 Differences in QSM cylinder sizes for a *Juglans nigra* (black walnut) tree and a showcase of the visualization tools of *rTwig*. a. is the unmodified, raw cylinder fits (*UnmodRadius)*, b. is parabolic QSM tapering from TreeQSM (*OldRadius)*, and c. is the Real Twig method (*radius*). d., e., and f. show a section of twigs overlaid on top of the input point cloud (pink) for each method. All panels were plotted with the *plot_qsm()* function.

3.2.3 Twig Database

Real Twig requires an input of the average twig size for a tree species to force the paths to end in realistically sized twigs. Twig characteristics are highly species and genus dependent (Fig. 3.2) and are unable to be accurately measured from point clouds due to the issues discussed in the introduction.

Twig measurements were generally lacking in published literature, so we created our own database of twig diameters, which is included in *rTwig*. The information contained in the database is shown in Table 3.1. A detailed description of our methods for measuring twigs can be found in Morales & MacFarlane (2024).

The twig database can be accessed by calling *twigs* once the *rTwig* library has been loaded, or *rTwig::twigs*, if just the twig database is desired from the package. See Table 3.1 for the components of the twig database. In addition to species specific twig measurements, we also include a genus average twig measurement, with a row labeled *Genus spp.* under the *scientific.name* column.

Column Name	Description
scientific.name	The tree's specific epithet
radius.mm	The average twig radius in millimeters
n	The total number of measurement samples
min	The smallest twig radius measurement
max	The largest twig radius measurement
std	The standard deviation
cv	The coefficient of variation

Table 3.1 Description of the twig database.

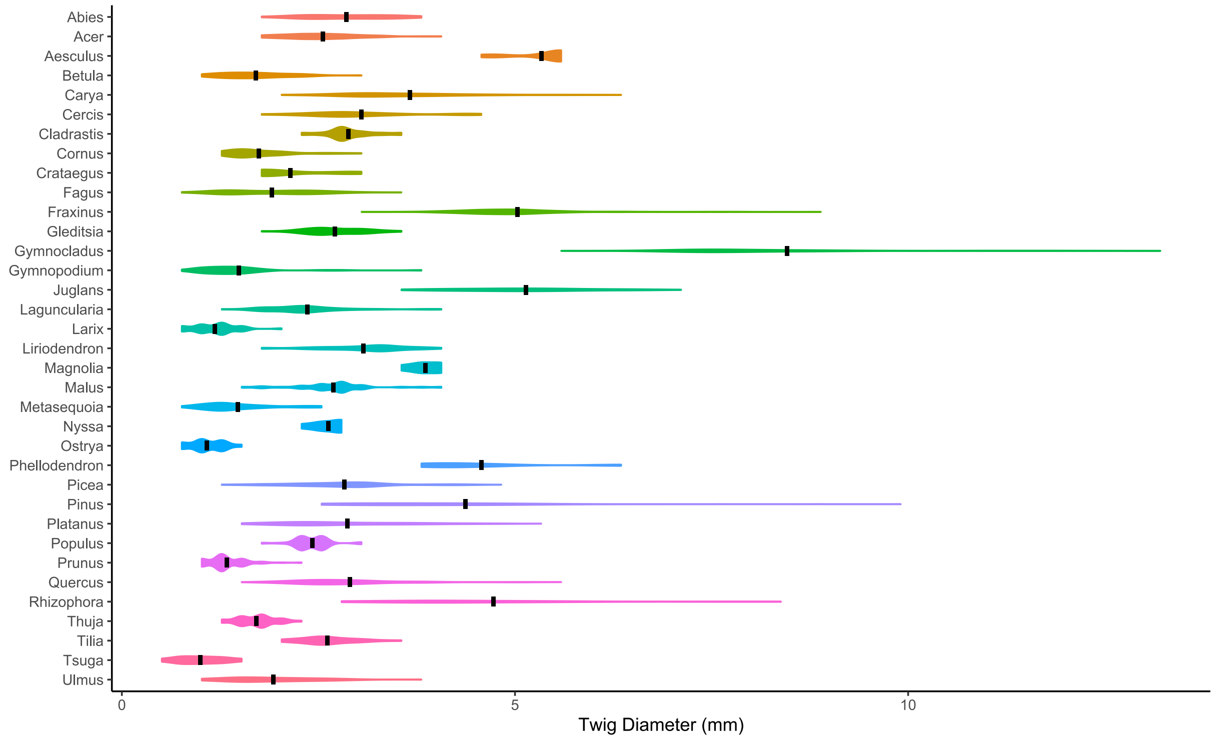

Figure 3.2 Measured twig diameter measurements across different tree genera showcasing twig diameter variability in the twigs database in *rTwig*. The black bar is the mean twig diameter in millimeters, while the line width and thickness show the distribution of diameters in millimeters. The colors represent the different genera shown on the y-axis.

3.3 rTwig Features and Example Tree

Users can install the initial public release version of *rTwig* from CRAN (v1.0.2, April 2024), or can install the latest development version from GitHub (https://github.com/aidanmorales/rTwig). Table 3.2 lists all the functions available in *rTwig* v1.0.2. A conceptual processing workflow with *rTwig* is shown in Figure 3.3. Figure 3.1 shows the QSM corrected with the Real Twig method and a closeup of the twig cylinders plotted against the input point cloud. To better understand and visualize the use of *rTwig* an example QSM *Juglans nigra* (black walnut) tree and example processing workflow with real data, code, and outputs is shown in Figure 3.4. Additional examples on how to use each function, function input parameters, vignettes, and package changelogs are available on our website (https://aidanmorales.github.io/rTwig/).

Function	**Description**
import_qsm	Imports a QSM created by TreeQSM (.mat extension)
update_cylinders	Standardizes cylinder relationships and calculates new variables
correct_radii	Models QSM paths and corrects cylinder radii overestimation
qsm_summary	Generates a summary of QSM diameter, height, volume, and surface area
smooth_qsm	Connects QSM cylinders end-to-end to smooth visualization
plot_qsm	Plots and individual QSM and (optionally) input point cloud
plot_stand	Plots multiple QSMs in the same plot and (optionally) their input point clouds
export_mesh	Exports a QSM as a mesh object (.ply extension)
export_mat	Exports a QSM (.mat extension) to be use in TreeQSM
box_dimension	Calculates and visualizes the structural complexity of a point cloud

Table 3.2 List of functions available in *rTwig*.

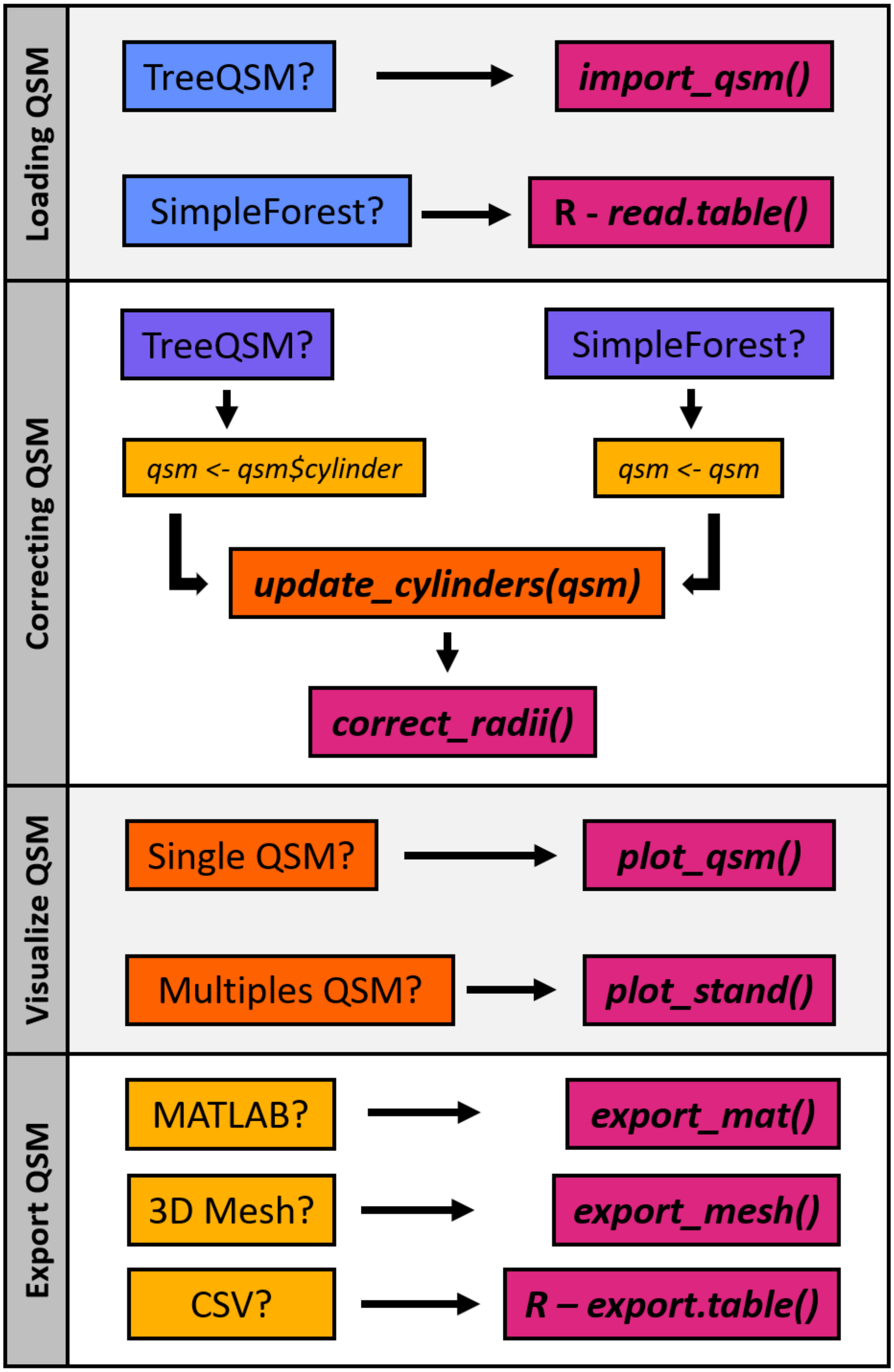

Figure 3.3 Schematic of an *rTwig* workflow. Each box represents the four main steps of processing a QSM produced with either TreeQSM or SimpleForest.

3.3.1 Importing a QSM

All *rTwig* functions operate on the QSM cylinder data, so importing the QSM cylinders into the R environment is the first step. The importing process changes depending on the software used to generate the QSM (Fig. 3.3). If the QSM output is in a standard format with delimiter-separated values, such as comma-separated values with SimpleForest QSMs, the user can import the QSM into R with their preferred function. If TreeQSM is used, the QSM is in a proprietary MATLAB (MathWorks, 2022) format. The *import_qsm()* function can be used to read in QSMs from TreeQSM. The user must specify the arguments of *file* (path to the QSM file) and *version* (version of TreeQSM). By default, *version* automatically detects the correct version for all publicly available versions of TreeQSM. However, the user can specify *version = "2.0"* if v2.0 of TreeQSM was used. In our example workflow (Fig. 3.4) we pass the QSM file (*BW13.mat*) as a string into the *file* parameter of *import_qsm()*. It is important to note that *import_qsm()* imports the six outputs of TreeQSM as an R *list* object. The QSM cylinder data is stored in the list object as an R *data.frame* with the name *cylinder*, which can be accessed with the extraction operator (e.g., *qsm$cylinder*, assuming the QSM is saved as an object called *qsm*). If we look at the output of *import_qsm()*, we see that the QSM is a list with six distinct elements, including our *cylinder data.frame* (Fig. 3.4).

3.3.2 Updating QSM Cylinder Data

Given the differences in how QSM data is stored between different QSM software, the QSM structure must be standardized to ensure the Real Twig method is consistent between all QSMs. We accomplished this with the *update_cylinders()* function. This function ensures consistent QSM topology (e.g., cylinder IDs, and branch ordering) and calculates new QSM variables if they are not already present. If TreeQSM is used, four new variables *growth length*, *reverse branch order*, *segment ID*, and *parent segment ID*, are calculated to match the outputs of SimpleForest. In our example workflow (Fig. 3.4), all we need to do is pass the *cylinder data.frame* into the *cylinder* parameter of the *update_cylinders()* function to ensure the QSM is in the proper structure. Updating the cylinders is a requirement to use any of the *rTwig* QSM functions and should always be done after importing a QSM into the R environment.

3.3.3 Correcting QSM Cylinder Radii

A species-specific twig radius is required to correct overestimated QSM cylinder radii of any given species using the Real Twig method. If the user has not measured a twig diameter, they can check the *twig* data base built into *rTwig* for their specific species (database described earlier). In our example, we extract the average twig radius for *Juglans nigra* (black walnut) by specifying the *scientific.name* in the *twigs* data base, which is 2.58 millimeters (Fig. 3.4). If the species is not present in the *twigs* data base, the genus radius average can serve as a substitute until a twig can be measured.

Once the twig diameter is known, the cylinder radii can be corrected using the *correct_radii()* function. The inputs are *cylinder* (the *cylinder data.frame*) and *radius* (the twig radius in millimeters), which in our example is 2.58 millimeters (Fig. 3.4). The final *correct_radii()* function parameter is *backend*. By default, *backend* is set to “multisession”, which is a parallel backend compatible with all platforms. If a Linux or MacOS system is used, *backend* can be set to “multicore” for less parallel overhead. If the user does not want to use parallel processing, or the overhead is greater than the processing time, *backend* can be set to “sequential”.

After running *correct_radii()*, there are three radii columns in the *cylinder data.frame* to choose from. *UnmodRadius* is the QSM cylinder radii without any modifications and is what the

Real Twig method uses by default. *OldRadius* the is QSM cylinder radii after any modifications made by the QSM software. Finally, *radius* is the QSM cylinder radii after being corrected with the Real Twig method. All three types of radii are visualized using our example *Juglans nigra* (black walnut) tree in Fig. 3.1.

3.3.4. QSM Summary

After correcting the radii, we can look at the QSM summary statistics with the *qsm_summary()* function. There are three input parameters for *qsm_summary()*. The first is *cylinder* (the *cylinder data.frame*). The second is *radius*, which defaults to “modified” (the radii after the Real Twig correction). Additional *radius* parameters are ”old” (*OldRadius*) and “unmodified” (*UnmodRadius*). The final input parameter is *triangulation,* which replaces the cylinder volume in the main stem up to the first branch with volume from a triangular mesh of the main stem, which only applies to QSMs made with TreeQSM. *triangulation* defaults to *FALSE*, but the user can supply the *triangulation list* imported with the *import_qsm()* function. In our *Juglans nigra* (black walnut) example (Fig. 3.4), we summarized the QSM statistics before and after running the Real Twig method. Before running Real Twig, the total tree volume was 2439 liters, and the total branch volume 1400 liters. After running Real Twig, the total tree volume was 1693 liters, and the total branch volume 649 liters. This is a 30.6% reduction in total tree volume, with nearly all the volume reduction occurring in the branches. This volume reduction is visualized in Fig. 3.1.

3.3.5 QSM Visualization and Export

rTwig also includes three functions for QSM visualization, and one function for exporting. All four of these functions take the *cylinder data.frame* as the main parameter in the *cylinder* input parameter. Additional input parameters are described in detail in the package documentation and example vignettes. *smooth_qsm()* ensures all cylinder endpoints are connected to improve visualization. Only TreeQSM is supported, as SimpleForest cylinder endpoints are already connected. *plot_qsm()* plots a single QSM, while *plot_stand()* plots multiple QSMs together in the same plot. Finally, *export_mat()* exports a QSM to the proprietary MATLAB format for use with TreeQSM.

```
# Load the rTwig Package
library(rTwig)

# Twig Radius for Juglans nigra
twigs[twigs$scientific.name == "Juglans nigra", ]
```

```
## # A data frame: 1 × 7
##   scientific.name radius.mm     n   min   max   std    cv
## * <chr>               <dbl> <dbl> <dbl> <dbl> <dbl> <dbl>
## 1 Juglans nigra        2.58    30  1.78  3.56  0.48  0.19
```

```
# Import a TreeQSM
qsm <- import_qsm(file = "BW13.mat")
summary(qsm)
```

```
##                Length Class      Mode
## cylinder       17     data.frame list
## branch         10     data.frame list
## treedata       83     -none-     list
## rundata        45     data.frame list
## pmdistance     21     -none-     list
## triangulation  0      -none-     list
```

```
# Update QSM & Correct Radii
qsm$cylinder <- update_cylinders(cylinder = qsm$cylinder)
qsm$cylinder <- correct_radii(cylinder = qsm$cylinder, twigRad = 2.58)

# QSM Summary Before Real Twig
qsm_summary(cylinder = qsm$cylinder, radius = "old")[[2]]
```

```
## # A tidytable: 1 × 8
##   QSM.dbh.cm QSM.ht.m Stem.vol.L Branch.vol.L Tot.vol.L Stem.sa.m2 Branch.sa.m2
##        <dbl>    <dbl>      <dbl>        <dbl>     <dbl>      <dbl>        <dbl>
## 1       42.1     17.7      1039.        1400.     2439.       13.0         140.
## # ℹ 1 more variable: Tot.sa.m2 <dbl>
```

```
# QSM Summary After Real Twig
qsm_summary(cylinder = qsm$cylinder, radius = "modified")[[2]]
```

```
## # A tidytable: 1 × 8
##   QSM.dbh.cm QSM.ht.m Stem.vol.L Branch.vol.L Tot.vol.L Stem.sa.m2 Branch.sa.m2
##        <dbl>    <dbl>      <dbl>        <dbl>     <dbl>      <dbl>        <dbl>
## 1       42.1     17.7      1044.         649.     1693.       12.9         64.9
## # ℹ 1 more variable: Tot.sa.m2 <dbl>
```

Figure 3.4 A typical *rTwig* workflow using a *Juglans nigra* (black walnut) tree generated with TreeQSM.

3.4 Limitations of rTwig

Our Real Twig method can correct QSM volume overestimation in small branches and twigs but makes several assumptions about cylinder fits and branch tapering. These assumptions generate precise and accurate estimates of total tree volume (Morales & MacFarlane, 2024) but may not always reflect the real taper within branches or main stem of a tree, depending on the quality of the input data.

Our method was trained with twig diameter measurements and does not incorporate measurements along the main stem or branches. As a result, what our method determines to be a good or bad cylinder fit may resize correct parts of the tree, especially in smaller diameter branches, leading to overaggressive tapering in smaller parts of the tree. Our method may also slightly increase the diameter of branch bases, especially if the branch base cylinder was determined to be a poor fit. Without enough good fit cylinders along the path, the GAM predicts the radius based on the closest good fit cylinders, which can inflate the branch base, and decrease the smaller branches, as the closest good fit cylinder for small branches is the measured twig diameter. These two assumptions create a branch taper that can be slightly inflated at the base and slightly too small towards the twig tip. These small errors cancel out and yield accurate branch volumes at the expense of the true taper. The greater the proportion of smaller branches a tree has the more apparent this becomes.

Based on internal testing of our method, this mainly affects excurrent growth forms with strong apical dominance. For such trees with abrupt changes in diameter along a path, some small branch cylinders may be labeled as bad fits. In contrast, decurrent growth forms without strong apical dominance have a more gradual drop in growth length between branches, with fewer small branch cylinders labeled as bad fits. Additionally, high-quality leaf-off conifer data sets with a range of species and sizes are not currently available for reference volume and biomass measurements. As a result, the current QSM correction functions in *rTwig* are best suited for decurrent growth forms and may underestimate small branch volume for trees with excurrent growth forms.

3.5 Summary

QSMs are a valuable tool to measure attributes of trees non-destructively and wholistically describe tree topology. We developed *rTwig* to improve and correct the widespread volume overestimation problem in QSMs, especially in small branches and twigs. *rTwig* not only corrects QSM volume overestimation, but it also provides a unique set of tools to analyze QSMs within the R ecosystem. We plan to improve the functionality of *rTwig* going forward and expand support for other QSM generation software. We also encourage users to submit bug reports, general contributions, and feature requests to our GitHub page (https://github.com/aidanmorales/rTwig/issues).

3.6 Software and Data Availability

Name of Software: rTwig

Package Developers: Aidan Morales, David W. MacFarlane

Type of Software: R package

First Available: 2024

Program Languages: R

Cost: Free

License: GPL 3

CRAN Repository https://cran.r-project.org/web/packages/rTwig/index.html

GitHub Repository: https://github.com/aidanmorales/rTwig

Install from CRAN: install.packages(‘‘rTwig’’)

Install Development Version: devtools::install_github("aidanmorales/rTwig")

Contact Information: Michigan State University, Forest Measurements and Modeling Lab, Department of Forestry, East Lansing, MI, USA

REFERENCES

Abegg, M., Kükenbrink, D., Zell, J., Schaepman, M. E., & Morsdorf, F. (2017). Terrestrial Laser Scanning for Forest Inventories-Tree Diameter Distribution and Scanner Location Impact on Occlusion. *Forests*. https://doi.org/10.3390/f8060184

Åkerblom, M., Raumonen, P., Mäkipää, R., & Kaasalainen, M. (2017). Automatic tree species recognition with quantitative structure models. *Remote Sensing of Environment*, *191*, 1–12. https://doi.org/10.1016/j.rse.2016.12.002

Arseniou, G., MacFarlane, D. W., Calders, K., & Baker, M. (2023). Accuracy differences in aboveground woody biomass estimation with terrestrial laser scanning for trees in urban and rural forests and different leaf conditions. *Trees - Structure and Function*. https://doi.org/10.1007/s00468-022-02382-1

Arseniou, G., MacFarlane, D. W., & Seidel, D. (2021). Woody Surface Area Measurements with Terrestrial Laser Scanning Relate to the Anatomical and Structural Complexity of Urban Trees. *Remote Sensing*, *13*(16), 3153. https://doi.org/10.3390/rs13163153

Barrett, T., Dowle, M., Srinivasan, A., Gorecki, J., Chirico, M., & Hocking, T. (2024). *data.table: Extension of `data.frame`*. https://r-datatable.com

Bengtsson, H. (2021). A Unifying Framework for Parallel and Distributed Processing in R using Futures. *The R Journal*, *13*(2), 208–227. https://doi.org/10.32614/RJ-2021-048

Bengtsson, H. (2022). *R.matlab: Read and Write MAT Files and Call MATLAB from Within R*. https://CRAN.R-project.org/package=R.matlab

Burt, A., Boni Vicari, M., Da Costa, A. C. L., Coughlin, I., Meir, P., Rowland, L., & Disney, M. (2021). New insights into large tropical tree mass and structure from direct harvest and terrestrial lidar. *Royal Society Open Science*, *8*(2), 201458. https://doi.org/10.1098/rsos.201458

Calders, K., Adams, J., Armston, J., Bartholomeus, H., Bauwens, S., Bentley, L. P., Chave, J., Danson, F. M., Demol, M., Disney, M., Gaulton, R., Krishna Moorthy, S. M., Levick, S. R., Saarinen, N., Schaaf, C., Stovall, A., Terryn, L., Wilkes, P., & Verbeeck, H. (2020). Terrestrial laser scanning in forest ecology: Expanding the horizon. *Remote Sensing of Environment*, *251*, 112102. https://doi.org/10.1016/J.RSE.2020.112102

Calders, K., Newnham, G., Burt, A., Murphy, S., Raumonen, P., Herold, M., Culvenor, D., Avitabile, V., Disney, M., Armston, J., & Kaasalainen, M. (2015). Nondestructive estimates of above-ground biomass using terrestrial laser scanning. *Methods in Ecology and Evolution*, 198–208. https://doi.org/10.1111/2041-210X.12301

Calders, K., Origo, N., Burt, A., Disney, M., Nightingale, J., Raumonen, P., Åkerblom, M., Malhi, Y., & Lewis, P. (2018). Realistic Forest Stand Reconstruction from Terrestrial LiDAR for Radiative Transfer Modelling. *Remote Sensing*, *10*(6), 933. https://doi.org/10.3390/rs10060933

Csárdi, G., Nepusz, T., Horvát, S., Traag, V., Zanini, F., & Noom, D. (2023). *igraph*. Zenodo. https://doi.org/10.5281/zenodo.7573267

Demol, M., Calders, K., Krishna Moorthy, S. M., Van den Bulcke, J., Verbeeck, H., & Gielen, B. (2021). Consequences of vertical basic wood density variation on the estimation of aboveground biomass with terrestrial laser scanning. *Trees*, *35*(2), 671–684. https://doi.org/10.1007/s00468-020-02067-7

Demol, M., Calders, K., Verbeeck, H., & Gielen, B. (2021). Forest above-ground volume assessments with terrestrial laser scanning: a ground-truth validation experiment in temperate, managed forests. *Annals of Botany*, *128*(6), 805–819. https://doi.org/10.1093/aob/mcab110

Demol, M., Verbeeck, H., Gielen, B., Armston, J., Burt, A., Disney, M., Duncanson, L., Hackenberg, J., Kükenbrink, D., Lau, A., Ploton, P., Sewdien, A., Stovall, A., Momo Takoudjou, S., Volkova, L., Weston, C., Wortel, V., Calders, K., & Alberto Silva, C. (2022). Estimating forest above-ground biomass with terrestrial laser scanning: Current status and future directions. *Methods Ecol Evol*, *13*, 1628–1639. https://doi.org/10.1111/2041-210X.13906

Demol, M., Wilkes, P., Raumonen, P., Krishna Moorthy, S., Calders, K., Gielen, B., & Verbeeck, H. (2022). Volumetric overestimation of small branches in 3D reconstructions of & Fraxinus excelsior; *Silva Fennica*, *56*(1), 10550. https://doi.org/10.14214/sf.10550

Disney, M. I., Boni Vicari, M., Burt, A., Calders, K., Lewis, S. L., Raumonen, P., & Wilkes, P. (2018). Weighing trees with lasers: Advances, challenges and opportunities. *Interface Focus*, *8*(2). https://doi.org/10.1098/rsfs.2017.0048

Fairbanks, M. (2024). *tidytable: Tidy Interface to 'data.table'*. https://markfairbanks.github.io/tidytable/, https://github.com/markfairbanks/tidytable.

Fan, G., Nan, L., Dong, Y., Su, X., & Chen, F. (2020). AdQSM: A New Method for Estimating Above-Ground Biomass from TLS Point Clouds. *Remote Sensing*, *12*(18), 3089. https://doi.org/10.3390/rs12183089

Gonzalez de Tanago, J., Lau, A., Bartholomeus, H., Herold, M., Avitabile, V., Raumonen, P., Martius, C., Goodman, R. C., Disney, M., Manuri, S., Burt, A., & Calders, K. (2018). Estimation of above-ground biomass of large tropical trees with terrestrial LiDAR. *Methods in Ecology and Evolution*, *9*(2), 223–234. https://doi.org/10.1111/2041-210X.12904

Hackenberg, J., & Bontemps, J.-D. (2023). Improving quantitative structure models with filters based on allometric scaling theory. *Applied Geomatics*, *15*(4), 1019–1029. https://doi.org/10.1007/s12518-023-00537-4

Hackenberg, J., Spiecker, H., Calders, K., Disney, M., Raumonen, P., Hyyppä, J., Liang, X., & Puttonen, E. (2015). *SimpleTree-An Efficient Open Source Tool to Build Tree Models from TLS Clouds*. *6*, 4245–4294. https://doi.org/10.3390/f6114245

Hackenberg, J., Wassenberg, M., Spiecker, H., & Sun, D. (2015). *Non Destructive Method for Biomass Prediction Combining TLS Derived Tree Volume and Wood Density*. *6*, 1274–1300. https://doi.org/10.3390/f6041274

Holopainen, M., Vastaranta, M., Kankare, V., Räty, M., Vaaja, M., Liang, X., Yu, X., Hyyppä, J., Hyyppä, H., Viitala, R., & Kaasalainen, S. (2012). BIOMASS ESTIMATION OF INDIVIDUAL TREES USING STEM AND CROWN DIAMETER TLS MEASUREMENTS. *The International Archives of the Photogrammetry, Remote Sensing and Spatial Information Sciences*, *XXXVIII-5/W12*, 91–95. https://doi.org/10.5194/isprsarchives-XXXVIII-5-W12-91-2011

MathWorks. (2022). *MATLAB* (9.13.0 (R2022b)). The MathWorks Inc. https://www.mathworks.com

Momo Takoudjou, S., Ploton, P., Sonké, B., Hackenberg, J., Griffon, S., de Coligny, F., Guy Kamdem, N., Libalah, M., II Mofack, G., Le Moguédec, G., Pélissier, R., & Barbier, N. (2018). Using terrestrial laser scanning data to estimate large tropical trees biomass and calibrate allometric models: A comparison with traditional destructive approach. *Methods of Ecolology and Evolution*, *9*, 905–916. https://doi.org/10.1111/2041-210X.12933

Morales, A., MacFarlane, D. W. (2024). Reducing Tree Volume Overestimation in Quantitative Structure Models Using Modeled Branch Topology and Direct Twig Measurements. Manuscript submitted for publication.

Murdoch, D., & Adler, D. (2024). *rgl: 3D Visualization Using OpenGL*.

Ng, P. T., & Maechler, M. (2022). *COBS – Constrained B-splines (Sparse matrix based)*. https://CRAN.R-project.org/package=cobs

R Core Team. (2024). *R: A Language and Environment for Statistical Computing*. https://www.R-project.org/

Raumonen, P., Kaasalainen, M., Akerblom, M., Kaasalainen, S., Kaartinen, H., Vastaranta, M., Holopainen, M., Disney, M., & Lewis, P. (2013). Remote Sensing Fast Automatic Precision Tree Models from Terrestrial Laser Scanner Data. *Remote Sens*, *5*, 491–520. https://doi.org/10.3390/rs5020491

Schlager, S. (2017). Morpho and Rvcg – Shape Analysis in R. In G. Zheng, S. Li, & G. Szekely (Eds.), *Statistical Shape and Deformation Analysis* (pp. 217–256). Academic Press.

Stovall, A. E. L., Vorster, A. G., Anderson, R. S., Evangelista, P. H., & Shugart, H. H. (2017). Non-destructive aboveground biomass estimation of coniferous trees using terrestrial LiDAR. *Remote Sensing of Environment*, *200*, 31–42. https://doi.org/10.1016/j.rse.2017.08.013

Terryn, L., Calders, K., Disney, M., Origo, N., Malhi, Y., Newnham, G., Raumonen, P., Åkerblom, M., & Verbeeck, H. (2020). Tree species classification using structural features derived from terrestrial laser scanning. *ISPRS Journal of Photogrammetry and Remote Sensing*, *168*, 170–181. https://doi.org/10.1016/j.isprsjprs.2020.08.009

Wickham, H., Averick, M., Bryan, J., Chang, W., McGowan, L. D., François, R., Grolemund, G., Hayes, A., Henry, L., Kuhn, J. H. and M., Pedersen, T. L., Miller, E., Bache, S. M., Müller, K., Ooms, J., Seidel, D. R. and D. P., Spinu, V., Takahashi, K., Vaughan, D., … Yutani, H. (2019). Welcome to the tidyverse. *Journal of Open Source Software*, *4*(43), 1686. https://doi.org/10.21105/joss.01686

Widgren, S., & Hulbert, C. (2023). *rmatio: Read and Write "Matlab" Files*. https://CRAN.R-project.org/package=rmatio

Wilkes, P., Lau, A., Disney, M., Calders, K., Burt, A., Gonzalez de Tanago, J., Bartholomeus, H., Brede, B., & Herold, M. (2017). Data acquisition considerations for Terrestrial Laser Scanning of forest plots. *Remote Sensing of Environment*, *196*, 140–153. https://doi.org/10.1016/j.rse.2017.04.030

Wilkes, P., Shenkin, A., Disney, M., Malhi, Y., Bentley, L. P., & Vicari, M. B. (2021). Terrestrial laser scanning to reconstruct branch architecture from harvested branches. Methods in Ecology and Evolution, 12(12), 2487–2500. https://doi.org/10.1111/2041-210X.13709

CHAPTER 4

SUMMARY AND RECOMMENDATIONS

4.1 Summary of Research

Our Real Twig method enables precise and accurate estimates of total tree volume and biomass from quantitative structure models (QSM) when species-specific twig diameters are supplied. QSMs corrected with our Real Twig method are visually realistic across a range of tree species (Fig. 2.1b, 2.1e, 2.1h, Fig. 3.1c). Furthermore, we tested our Real Twig method against high-quality reference destructive sampling data and point cloud data of various quality, collected with both time-of-flight (TOF) and phase-shift (PS) laser scanning sensors. Across our 41 study trees, we found that our Real Twig method consistently produced total tree QSM volumes and mass within ± 10% of the reference data. Based on these results, we are confident that Real Twig can produce precise and accurate estimates of total tree volume without the need for reference destructive sampling data. However, careful judgment is required to generate topologically correct input point clouds and QSMs for the best possible results using Real Twig.

We found that QSM small branch and twig volume overestimation depends on two main factors. First, volume overestimation is directly proportional to the size of the tree, the total number of twigs in a tree, and the species-specific twig diameter (Table 2.3, Fig. 2.6). The larger the species-specific twig diameter, the less the twig is affected by wind noise, beam divergence, and co-registration errors, leading to lower QSM volume overestimation, with the converse being true for trees with smaller twig diameters. Similarly, the topology of the QSM has a significant effect on volume overestimation or underestimation of small branches and twigs (Fig. 2.7). If the QSM fails to reconstruct large portions of small branches and twigs from a point cloud or does not reconstruct cylinders all the way to the end of the twig, compensatory errors and volume omission may mask small branch volume overestimation.

These findings agree with and provide a new explanation for the varying results of previous QSM volume validation studies. Species-specific twig diameters can explain QSM volume overestimation between different species with everything else held constant. For example, Demol et al. (2021) found that European larch (*Larix decidua*), which has an average twig diameter around one millimeter (Fig. 3.2), had QSM volumes over double that of the reference data, while European beech and European ash (*Fagus sylvatica*, *Fraxinus excelsior*) with larger twig diameters (Fig. 3.2) had less than 39% volume overestimation. Similarly, different QSM software versions can drastically affect volume estimates. Using TreeQSM v2.4 on two different European ash trees, Demol et al. (2022) found QSM volume was overestimated by 45% on average, compared to an average overestimation of 38% using TreeQSM v2.3, when scanned and destructively sampled following the same protocol on 15 different European ash trees (Demol et al., 2021). Finally, the size of the tree and twig diameter can explain the relative amount of QSM volume overestimation. For example, the four large tropical trees (Burt et al., 2021) showed the lowest overall error without Real Twig applied and have large twig diameters ~1 cm in size, while the smallest red maple from Harvard Forest had > 400% total mass overestimation and has twig diameters ~5 times smaller than the tropical trees (Table 2.3, Fig. 2.6).

4.2 Recommendations

4.2.1 Twig Measurements

Given the importance of twig diameter measurements for correcting QSM volume overestimation, we have the following recommendations for measuring twig diameters for different species. First, we recommend collecting a minimum of 30 twig diameters for each tree species to ensure tree-to-tree variation is sufficiently captured. Samples should be collected from individual trees of various sizes whenever possible. As Wilkes et al. (2021) suggested, we also recommend collecting a maximum of ≤ 5 twigs from an individual tree to ensure that no individual can bias the species-specific average twig diameter. If a tree is destructively sampled for mass validation, we recommend collecting ≤ 5 twig measurements from each branch coming off the main stem. If the same species is present or has been introduced across continents, we recommend collecting additional twig measurements to assess whether twig diameters vary by species across wide geographic ranges.

We also recommend measuring twig diameters during the dormant season when possible. In temperate climates, this is between late fall and early spring, when deciduous trees have lost their leaves, but before their buds begin to break. In tropical and subtropical climates this may occur during the dry or rainy season depending on the species. Measuring twigs during the dormant season ensures that we capture the twig after it has finished growing for the season and do not underestimate its diameter by measuring the region of active twig growth.

If not cost or time prohibited, we also recommend collecting additional ecological data related to the twig diameter, such as tree form, leaf morphology, position in the canopy, relative position of the measured twig in the canopy, and diameter measurements for a subset of branches to compare to the QSM. These variables would enhance a twig measurements data set beyond simple diameter measurements, and provide the scientific community with a novel, rich data set to better understand the role of twigs within individual trees, different species, and their response to different environmental conditions. This data would also be invaluable for benchmarking improvements in TLS sensor technology and QSM topology over time.

4.2.2 TLS Sensor Characteristics and Twigs

QSMs and their ability to accurately resolve fine branching structures can only be as good as their input point cloud data. If the input point cloud does not represent the tree well, the QSM cannot model the tree well. Consequently, the effectiveness of our Real Twig method to correct QSM branch taper is also dependent on point cloud quality. Therefore, we strongly recommend using the twig diameter of a tree as the focus for TLS data collection and matching the TLS sensor to the site conditions and desired goals.

The first consideration is the type of TLS sensor and its characteristics used to collect the point cloud data, with phase-shift (PS) and time-of-flight (TOF) being the two main sensors used in forestry applications. The ability of TOF sensors to emit discreet laser pulses with high signal-to-noise ratios and multiple returns per pulse over hundreds of meters (in the case of the Riegl VZ series), gives TOF a distinct advantage over PS scanners, with limited ranges, single returns, and low signal-to-noise ratios, especially around the edges of objects (Calders et al., 2020). However, PS scanners have much lower beam divergence, smaller exit beam diameters, lower ranging error, and faster data acquisition rates than TOF sensors, making them more suitable for resolving fine details within 100 meters with higher accuracy (Suchocki, 2020). Considering these sensor specific characteristics against known twig diameters helps to explain the small branch overestimation in point clouds. The ranging error (the measured distance versus the true distance from the sensor) for typical PS sensors is ± 2 mm, and ± 5 mm for TOF sensors (Suchocki, 2020), which is larger than most twig diameters (Fig. 3.2). As Stovall et al. (2023) showed, lower ranging errors and exit beam diameters dramatically increase a sensor’s ability to accurately resolve small parts of a tree. Until the ranging error is less than the twig diameter, current TLS sensors will always overestimate the width of twigs in point clouds.

4.2.3 Angular Resolution and Twigs

The angular resolution of the scanner, the angle in degrees between subsequent vertical scan lines, is perhaps more important than the ranging error, as ranging error only occurs when a laser pulse intercepts an object and can record a return. If the angular resolution of the scanner is wider than the twig diameter at a given distance, and any part of the beam footprint does not intercept the twig, no point will be recorded for the twig. However, if a laser pulse intercepts a twig, but the center of the laser pulse does not fully contain the twig, the recorded data will have a weak signal with low accuracy and inflate the twig diameter even further (Wilkes et al., 2021). This effect is most noticeable on small diameter parts of a tree, but it occurs to varying degrees whenever the laser footprint is wider than the part of the tree it intersects.

Over the past decade of TLS forestry campaigns, an angular resolution of 0.04° – 0.06° with a spacing of 10 meters between subsequent scans has been widely used to balance scan number and post-processing time versus data acquisition rate and data quality (Wilkes et al., 2017). However, if we consider angular resolution against the twig diameter, too high of an angular resolution quickly degrades the point cloud quality as distance from the scanner increases. Morhart et al. (2024) demonstrated this problem well; using a Riegl-VZ 400i with an angular resolution of 0.04° to scan branches in a controlled environment, the spacing between each laser pulse was 3 millimeters when the scanner was placed 5 meters away from the branch, and 1.4 centimeters when the scanner was placed 20 meters away from the branch, with point cloud and QSM quality quickly degrading as distance from the scanner increased. Given a typical twig diameter (Table 3.2) and a typical twig height above the ground 20 meters from the scanner, with an angular resolution of 0.04°, the point spacing (~ 1 centimeter) is much larger than the twig diameter depending on the sensor specific beam divergence characteristics. The points that are captured are unlikely to have the center of the laser pulse intercept a twig directly, leading to poor point cloud accuracy. However, the relationship between angular resolution and point spacing is linear at any given distance (assuming a fixed angle of incidence), so halving the angular resolution doubles the point spacing, and vice versa. Lowering the angular resolution ensures more laser pulse centroids directly intercept the tree at any given distance, leading to increased point cloud accuracy for smaller parts of the tree at the expense of oversampling larger portions of the tree.

Based on our results using Real Twig, we found that lower angular resolutions significantly improve both the twigs in the point cloud and the QSM. For example, the tree shown in Fig. 3.1 was scanned with a Faro Focus3D X 330 scanner with angular resolutions between 0.009° and 0.018° as part of a 20 x 60 meter plot of 50 trees following the protocol described in Wilkes et al. (2017). As shown in Fig. 3.1, the resulting point cloud and QSM replicate the branching structure and twigs well. We believe that the tradeoff of increased storage space and scan time with lower angular resolutions is worth the better point cloud and QSM quality.

4.2.4 Final Recommendations and Future Work

Our Real Twig method corrects QSM volume overestimation, and our twig diameter measurements provide new insights into TLS data collection of trees. To ensure the best possible results with Real Twig, we recommend collecting species-specific twig diameter measurements and the highest quality point cloud with twigs resolved as finely as possible. Until a satisfactory way to filter phase-shift sensor noise exists, we recommend using time-of-flight sensors, due to their superior signal-to-noise ratio and ability to record multiple returns with high accuracy, which is especially important for collecting data in complex or leaf-on forest conditions. We recommend optimizing the angular resolution of the scanner to fully contain points along the twig depending on the height of the canopy and the diameter of the twig. Finally, we recommend carefully selecting input parameters and inspecting the final QSM, to ensure the topology of the QSM best represents the real tree.

We see three main objectives for future work. First, future studies should compare multiple laser scanning sensors and their ability to resolve twigs and small branches. These studies should compare time-of-flight and phase-shift sensors across different distances and angular resolutions versus manual small branch measurements to quantify sensor-specific small branch overestimation. Second, they should consider how much sensor-specific small branch and twig overestimation Real Twig can correct from the QSM, including a sensitivity analysis using the full range of species-specific twig diameters. Finally, the results of these studies can be used to improve the Real Twig method even further, ensuring precise and accurate branch tapering across a range of laser scanning sensors and tree species. Work is underway with the *rTwig* package to not only support more QSM software, but also rewrite core functions using *Rcpp*, (Eddelbuettel & Balamuta, 2018), a high performance C++ backend for R. A better understanding of laser scanning sensors, small branch and twig measurements, and high performance software, will not only improve non-destructive tree measurements, but also deepen our understanding of real trees.

REFERENCES

Burt, A., Boni Vicari, M., Da Costa, A. C. L., Coughlin, I., Meir, P., Rowland, L., & Disney, M. (2021). New insights into large tropical tree mass and structure from direct harvest and terrestrial lidar. *Royal Society Open Science*, *8*(2), 201458. https://doi.org/10.1098/rsos.201458

Calders, K., Adams, J., Armston, J., Bartholomeus, H., Bauwens, S., Bentley, L. P., Chave, J., Danson, F. M., Demol, M., Disney, M., Gaulton, R., Krishna Moorthy, S. M., Levick, S. R., Saarinen, N., Schaaf, C., Stovall, A., Terryn, L., Wilkes, P., & Verbeeck, H. (2020). Terrestrial laser scanning in forest ecology: Expanding the horizon. *Remote Sensing of Environment*, *251*, 112102. https://doi.org/10.1016/J.RSE.2020.112102

Demol, M., Calders, K., Verbeeck, H., & Gielen, B. (2021). Forest above-ground volume assessments with terrestrial laser scanning: a ground-truth validation experiment in temperate, managed forests. *Annals of Botany*, *128*(6), 805–819. https://doi.org/10.1093/aob/mcab110

Demol, M., Wilkes, P., Raumonen, P., Krishna Moorthy, S., Calders, K., Gielen, B., & Verbeeck, H. (2022). Volumetric overestimation of small branches in 3D reconstructions of & Fraxinus excelsior; *Silva Fennica*, *56*(1), 10550. https://doi.org/10.14214/sf.10550

Eddelbuettel, D., & Balamuta, J. J. (2018). Extending *R* with C++: A Brief Introduction to Rcpp. *The American Statistician*, *72*(1), 28–36. https://doi.org/10.1080/00031305.2017.1375990

Morhart, C., Schindler, Z., Frey, J., Sheppard, J. P., Calders, K., Disney, M., Morsdorf, F., Raumonen, P., & Seifert, T. (2024). Limitations of estimating branch volume from terrestrial laser scanning. *European Journal of Forest Research*, *143*(2), 687–702. https://doi.org/10.1007/s10342-023-01651-z

Stovall, A. E., MacFarlane, D. W., Crawford, D., Jovanovic, T., Frank, J., & Brack, C. (2023). Comparing mobile and terrestrial laser scanning for measuring and modelling tree stem taper. *Forestry: An International Journal of Forest Research*, *96*(5), 705–717. https://doi.org/10.1093/forestry/cpad012

Suchocki, C. (2020). Comparison of Time-of-Flight and Phase-Shift TLS Intensity Data for the Diagnostics Measurements of Buildings. *Materials*, *13*(2), 353. https://doi.org/10.3390/ma13020353

Wilkes, P., Lau, A., Disney, M., Calders, K., Burt, A., Gonzalez de Tanago, J., Bartholomeus, H., Brede, B., & Herold, M. (2017). Data acquisition considerations for Terrestrial Laser Scanning of forest plots. *Remote Sensing of Environment*, *196*, 140–153. https://doi.org/10.1016/j.rse.2017.04.030

Wilkes, P., Shenkin, A., Disney, M., Malhi, Y., Bentley, L. P., & Vicari, M. B. (2021). Terrestrial laser scanning to reconstruct branch architecture from harvested branches. *Methods in Ecology and Evolution*, *12*(12), 2487–2500. https://doi.org/10.1111/2041-210X.13709